The background of the slide is a complex, fractal-like visualization of point events. It consists of a dense, branching network of red and green lines and dots, resembling a biological structure like a neuron or a communication network. The overall color palette is dominated by red, green, and black, with some lighter green and yellowish areas. The structure is highly irregular and self-similar, characteristic of fractal geometry.

Fractal Point Events in Physics, Biology, and Communication Networks

Malvin Carl Teich
Boston University
<http://people.bu.edu/teich>

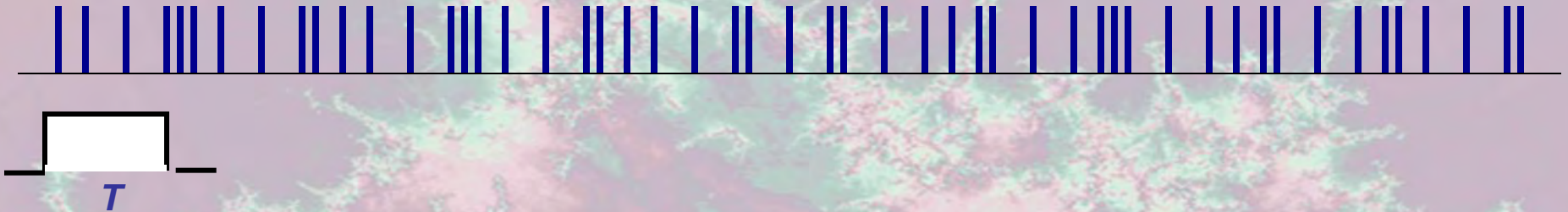
1. OUTLINE

1. OUTLINE
2. POINT EVENTS
3. FRACTALS AND FRACTAL POINT EVENTS
4. FRACTAL PHOTONS
5. HEART RATE VARIABILITY
6. NETWORKS
7. SENSORY DETECTION

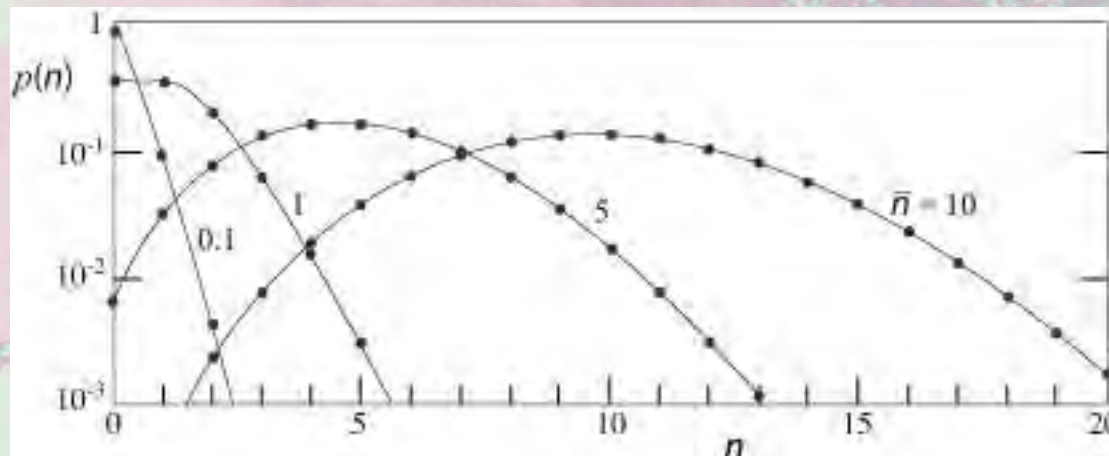
2. POINT EVENTS

COUNTING POINT EVENTS IN A FIXED TIME WINDOW T

Poisson process (zero-memory):



For this process, the counting distribution $p(n)$ (i.e., the relative frequency or probability mass function) for the number of events n is characterized by the Poisson distribution, $p(n) = (\lambda T)^n e^{-\lambda T} / n!$, whose variance-to-mean ratio F is unity, so $\text{var}(n) \equiv \sigma^2 = \bar{n} = \lambda T$:



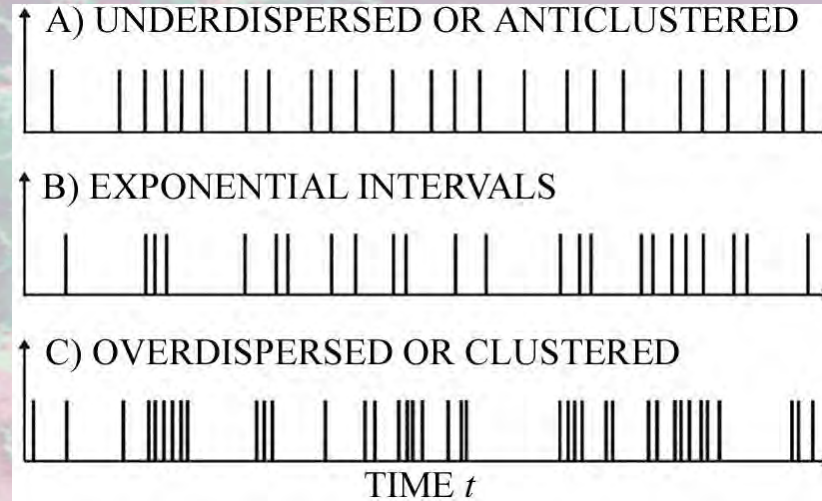
Poisson



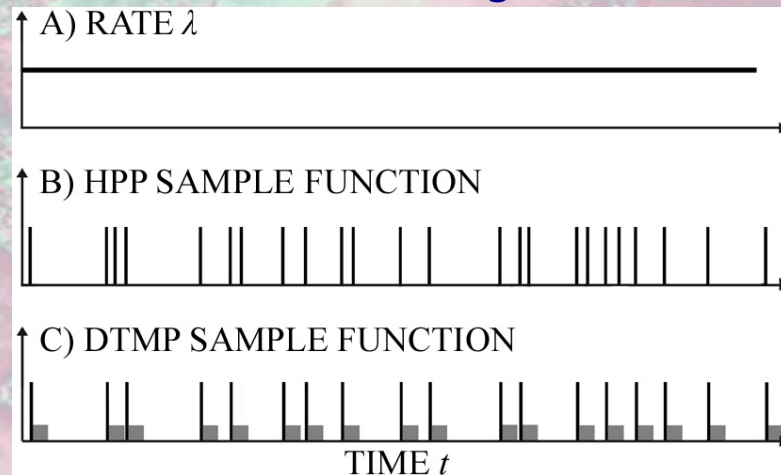
After Saleh and Teich, *Fundamentals of Photonics*,
2nd Ed. (Wiley, 2007), Chap. 12.

ANTICLUSTERED AND CLUSTERED POINT EVENTS

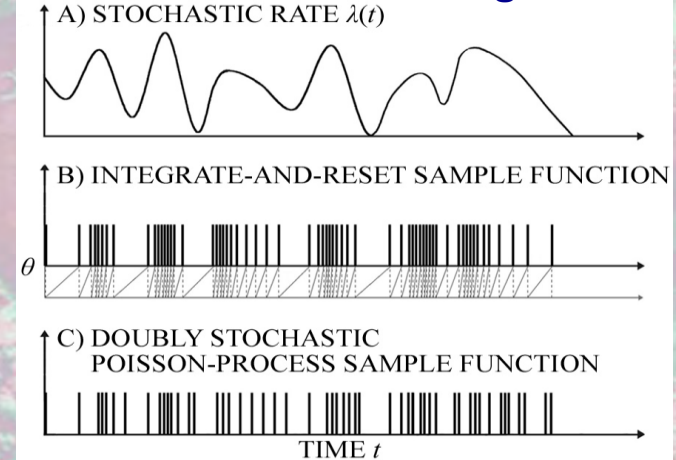
HPP:



Dead-time anticlustering:



Rate-variation clustering:

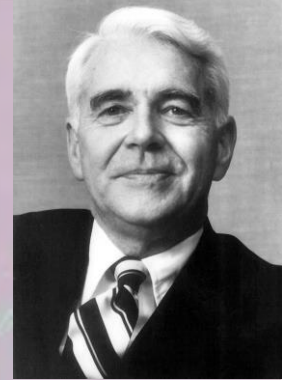


Cox



**IMPORTANT EXAMPLES OF ANTICLUSTERED EVENTS VIA DEAD-TIME-MODIFICATION.
 IMPORTANT EXAMPLES OF CLUSTERED EVENTS: NEGATIVE-BINOMIAL (NB) AND
 NEYMAN TYPE-A (NTA) DISTRIBUTIONS, AND VARIATIONS THEREOF**

NEURAL COUNTING AND PHOTON COUNTING



McGill

W. J. McGill, "Signal Detection Theory," presented at the *University Seminar on Mathematical Methods in the Social Sciences*, Columbia University, March 1974.

VOLUME 36, NUMBER 13

PHYSICAL REVIEW LETTERS

29 MARCH 1976

Neural Counting and Photon Counting in the Presence of Dead Time*

Malvin Carl Teich† and William J. McGill
Columbia University, New York, New York 10027
(Received 10 November 1975)

The usual stimulus-based neural counting model for audition is found to be mathematically identical to the well-known semiclassical formalism for photon counting. In particular, we explicitly demonstrate the equivalence of McGill's noncentral negative binomial distribution and Peřina's multimode confluent hypergeometric distribution for a coherent signal imbedded in chaotic noise. Dead-time corrections, important both in neural counting and in photon counting, are incorporated in a generalized form of this distribution. Some specific implications of these results are discussed.

NTA DISTRIBUTION – NEURAL EVENTS

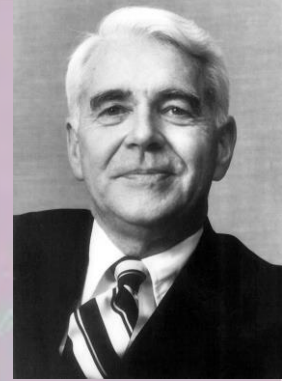
Reprinted from JOURNAL OF MATHEMATICAL PSYCHOLOGY
All Rights Reserved by Academic Press, New York and London

Vol. 4 No 3, October 1967
Printed in Belgium

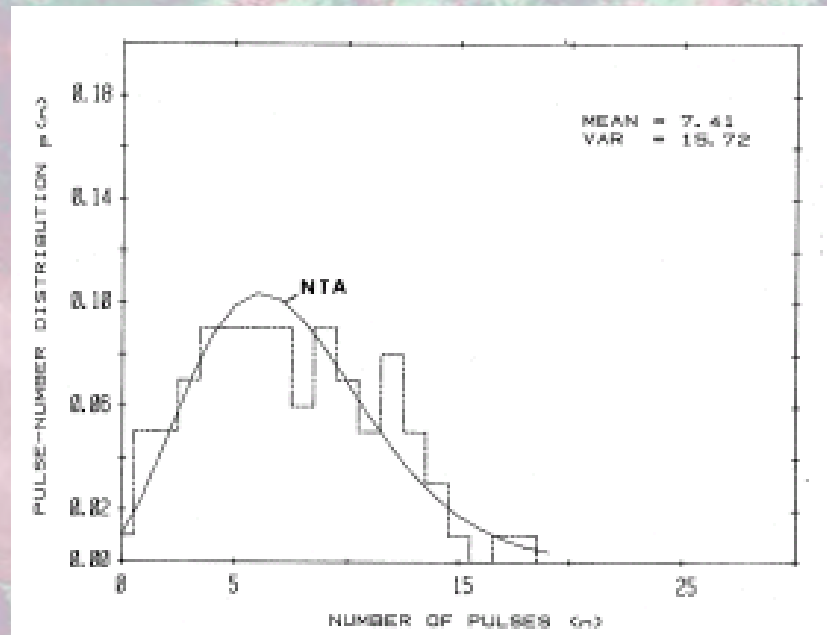
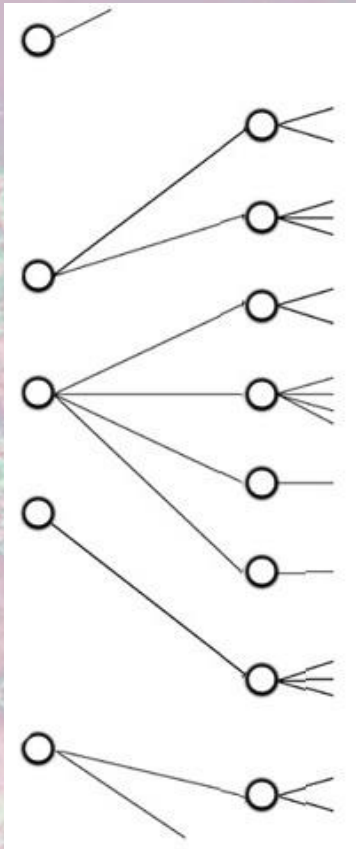
Neural Counting Mechanisms and Energy Detection in Audition

WILLIAM J. MCGILL

University of California San Diego, California 92037



McGill



After Saleh and Teich, "Multiplication and Refractoriness in the Cat's Retinal-Ganglion-Cell Discharge at Low Light Levels,"
Biol. Cybern. **52**, 101-107 (1985).

NEYMAN TYPE-A DISTRIBUTION – BUGS

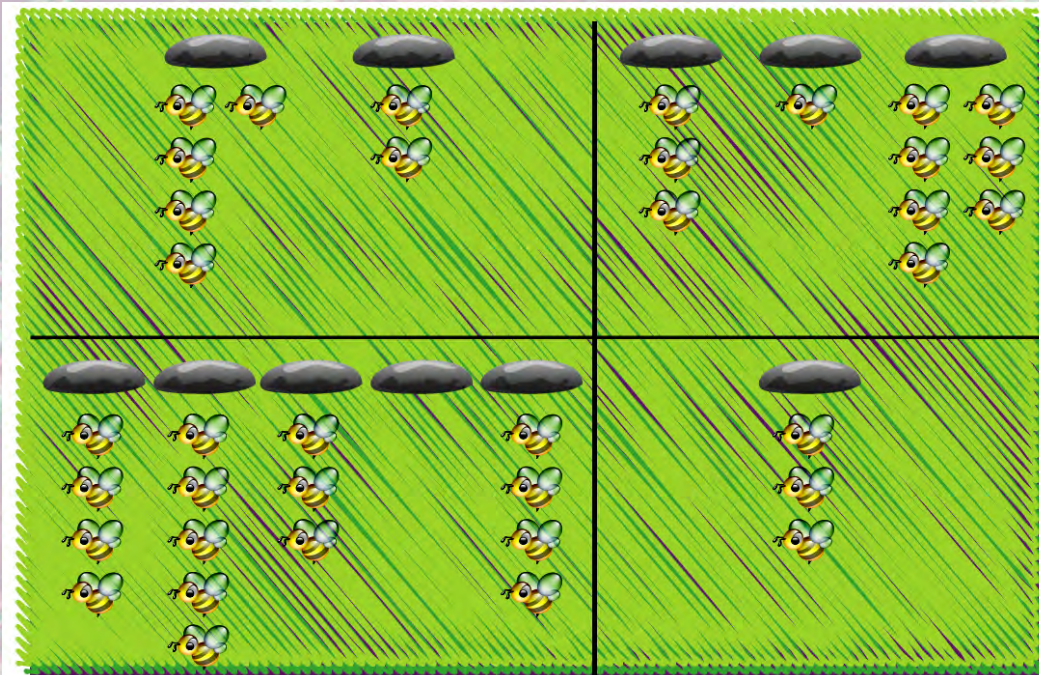
On a New Class of "Contagious" Distributions, Applicable in Entomology and Bacteriology

J. Neyman

The Annals of Mathematical Statistics, Vol. 10, No. 1 (Mar., 1939), 35-57.



Neyman



$$p(n) = \sum_{m=0}^{\infty} p(n|m)p(m)$$
$$= \sum_{m=0}^{\infty} \frac{(\alpha m)^n e^{-\alpha m}}{n!} \frac{\langle m \rangle^m e^{-\langle m \rangle}}{m!}$$
$$p(0) = \exp\left[-\langle m \rangle(1 - e^{-\alpha})\right]$$

NTA DISTRIBUTION – VISUAL PERCEPTION

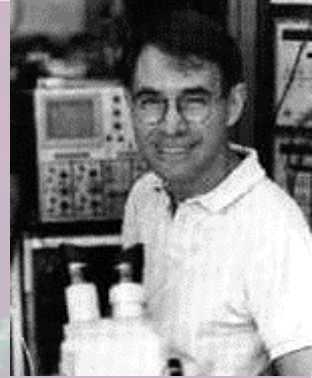
Photon Counting and Energy Detection in Vision

Malvin Carl Teich and Paul R. Prucnal

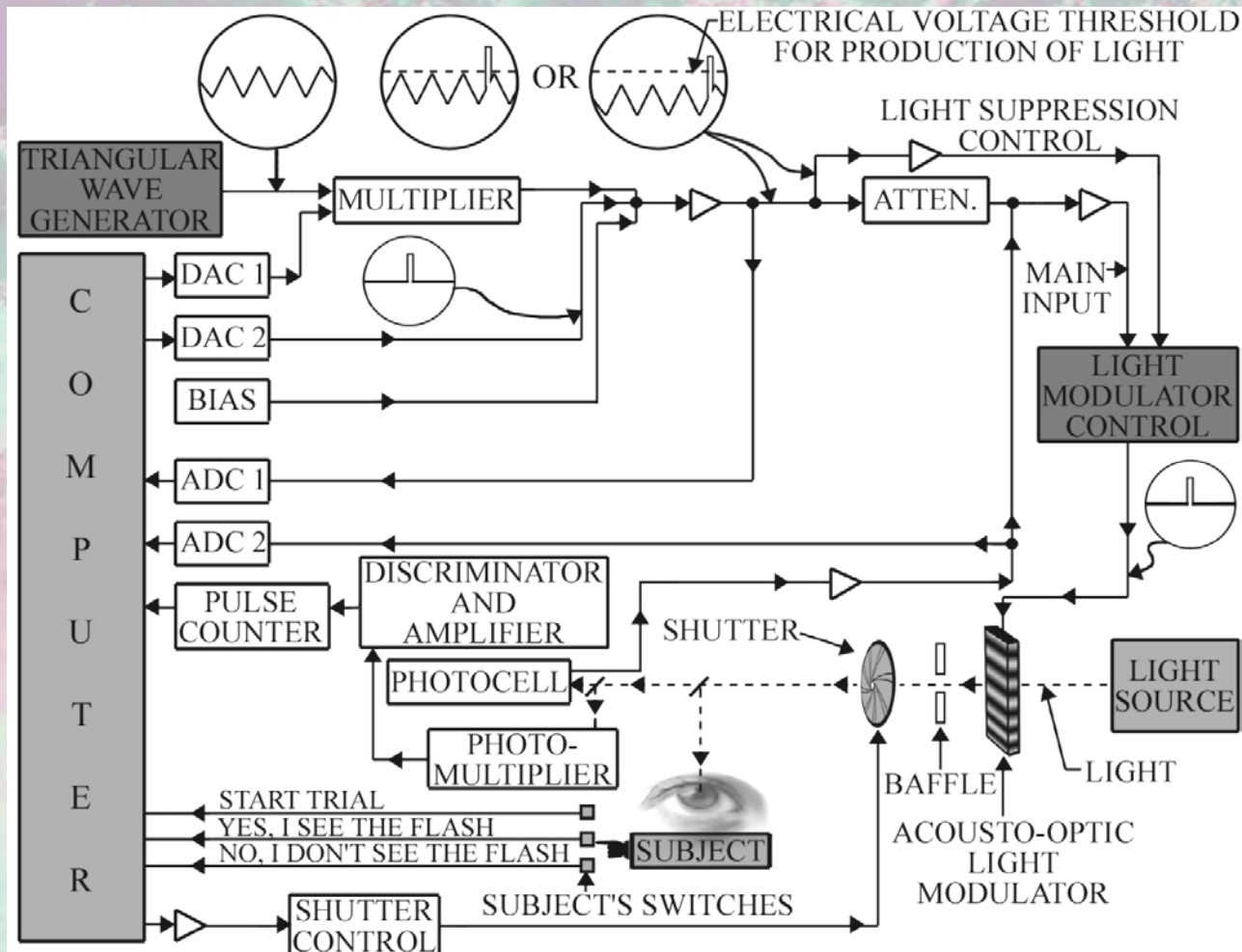
Department of Electrical Engineering and Computer Science, Columbia University, New York, New York 10027

J. Opt. Soc. Am., Vol. 67, No. 10, October 1977

Copyright © 1977 by the Optical Society of America



Prucnal

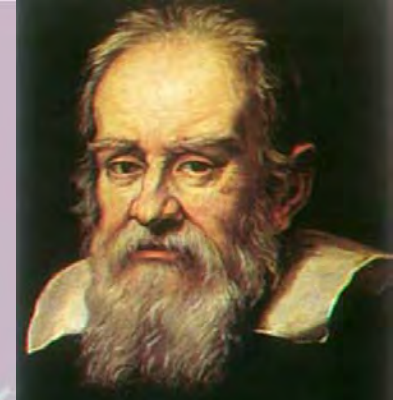


NTA DISTRIBUTION – PHOTONS

IEEE JOURNAL OF QUANTUM ELECTRONICS, VOL. QE-17, NO. 12, DECEMBER 1981

Discrimination of Shot-Noise-Driven Poisson Processes by External Dead Time: Application to Radioluminescence from Glass

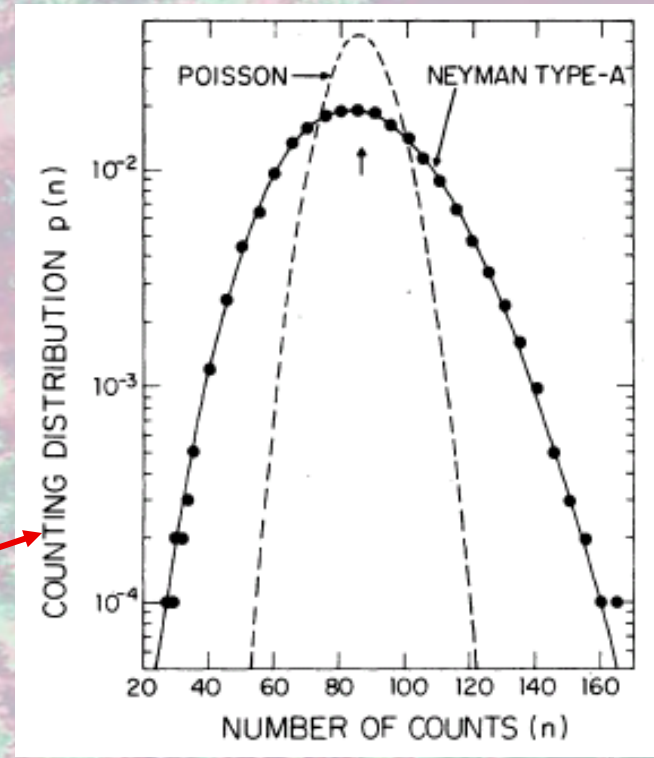
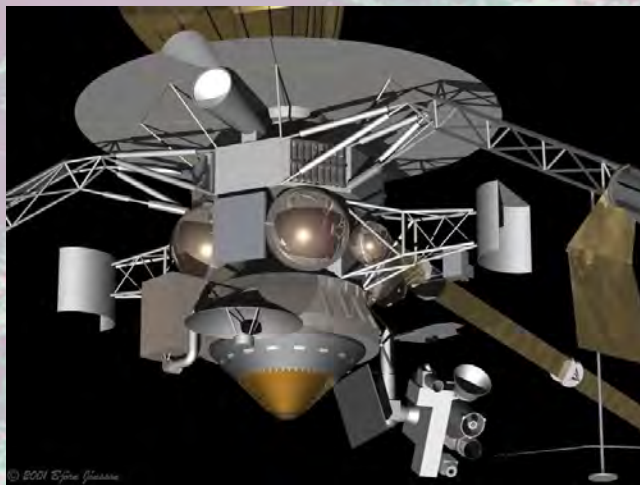
BAHAA E. A. SALEH, MEMBER, IEEE, JOSEPH T. TAVOLACCI, MEMBER, IEEE, AND MALVIN CARL TEICH, SENIOR MEMBER, IEEE



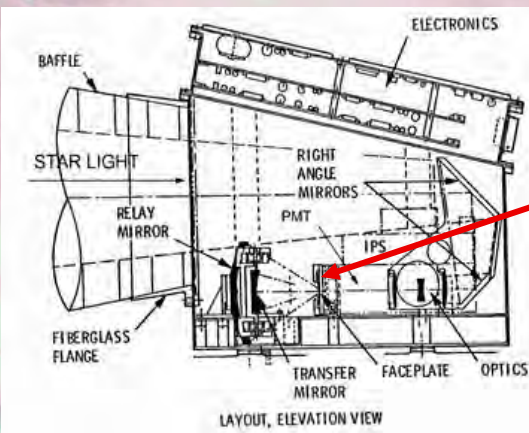
Galileo

GALILEO MISSION TIMELINE:

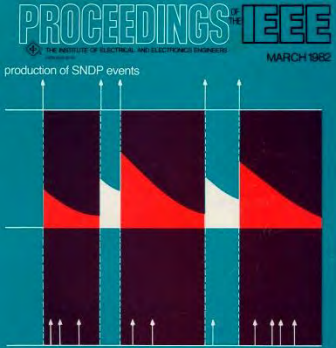
IDEA: Oct. 1977
LAUNCH: Oct. 1989
ARRIVAL: Dec. 1995
DEATH: Sep. 2003
PHOTOS: 14,000
DATA: 30 Gbytes



**PMT FACEPLATE
 BETALUMINESCENCE**



After Teich and Saleh, "Fluctuation Properties of Multiplied-Poisson Light: Measurement of the Photon-Counting Distribution for Radioluminescence Radiation from Glass," *Phys. Rev. A* **24**, 1651-1654 (1981).

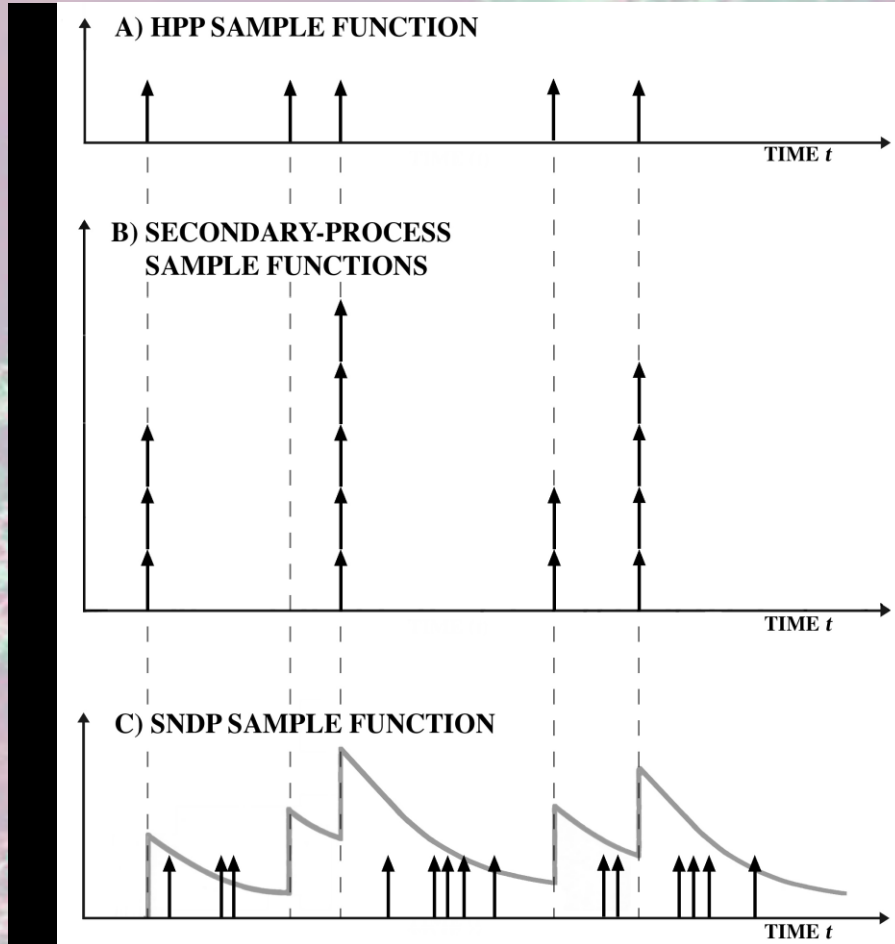


NTA DISTRIBUTION – SHOT-NOISE-DRIVEN POISSON

PROCEEDINGS OF THE IEEE, VOL. 70, NO. 3, MARCH 1982

Multiplied-Poisson Noise in Pulse, Particle, and Photon Detection

BAHAA E. A. SALEH, MEMBER, IEEE, AND MALVIN CARL TEICH, SENIOR MEMBER, IEEE



CASCADE VARIANCE THEOREM

$$\langle n \rangle = \langle \alpha \rangle \langle m \rangle$$

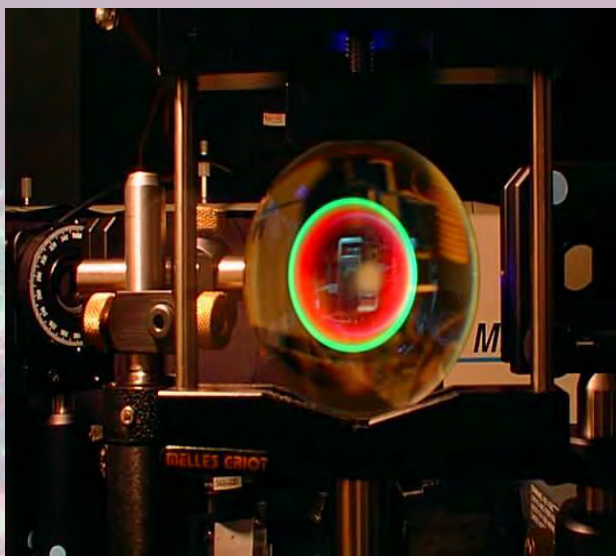
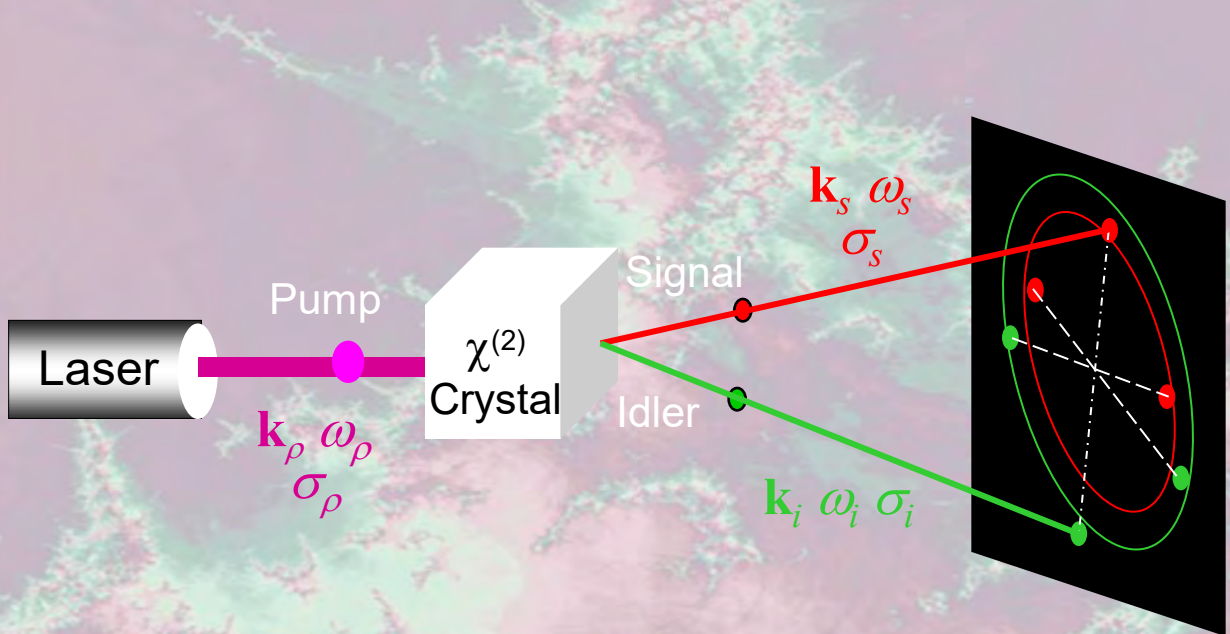
$$\text{var}(n) = \langle \alpha \rangle^2 \text{var}(m) + \langle m \rangle \text{var}(\alpha)$$

$$F_n \equiv \frac{\text{var}(n)}{\langle n \rangle} = \langle \alpha \rangle F_m + F_\alpha$$

for $F_m = F_\alpha = 1$:

$$F_n = 1 + \langle \alpha \rangle \quad (\text{NTA})$$

GENERATING PAIRS OF POINT EVENTS VIA SPONTANEOUS PARAMETRIC DOWN-CONVERSION: ENTANGLED PHOTONS

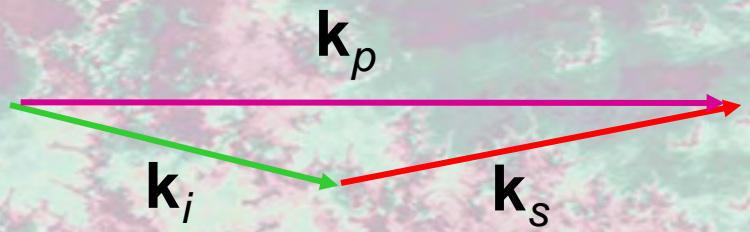


Conservation of energy

$$\omega_\rho = \omega_s + \omega_i$$

Conservation of momentum

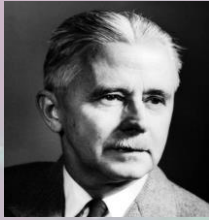
$$\mathbf{k}_\rho = \mathbf{k}_s + \mathbf{k}_i$$



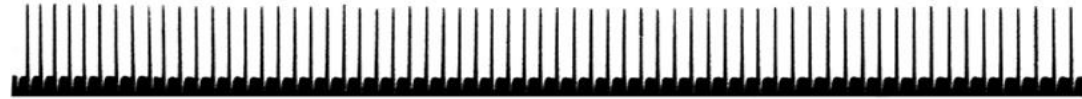
Adapted from Joobeur, Saleh, and Teich, "Spatiotemporal Coherence Properties of Entangled Light Beams Generated by Parametric Down-Conversion," *Phys. Rev. A* **50**, 3349-3361 (1994).

RANDOM POINT EVENTS IN NEUROPHYSIOLOGY

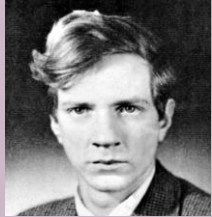
Hartline



A) *LIMULUS* AFFERENT OPTIC-NERVE-FIBER DISCHARGE



Barlow
Levick



B) CAT RETINAL-GANGLION-CELL MAINTAINED DISCHARGE



Davis
Tasaki



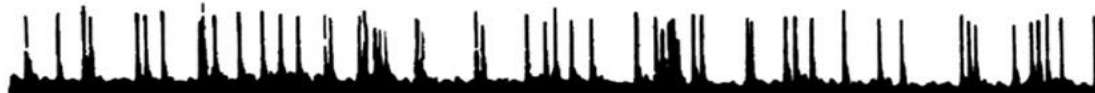
C) CAT AUDITORY-NERVE-FIBER SPONTANEOUS DISCHARGE



Kuffler



D) CAT RETINAL-GANGLION-CELL SPONTANEOUS DISCHARGE



Evarts



E) MONKEY PYRAMIDAL-TRACT SLEEP DISCHARGE



1 sec

COUNTING STATISTICS FOR POINT EVENTS IN THE MAMMALIAN AUDITORY SYSTEM

1110 J. Acoust. Soc. Am. 77 (3), March 1985 0001-4966/85/031110-19\$00.80 © 1985 Acoustical Society of America 1110

Pulse-number distribution for the neural spike train in the cat's auditory nerve

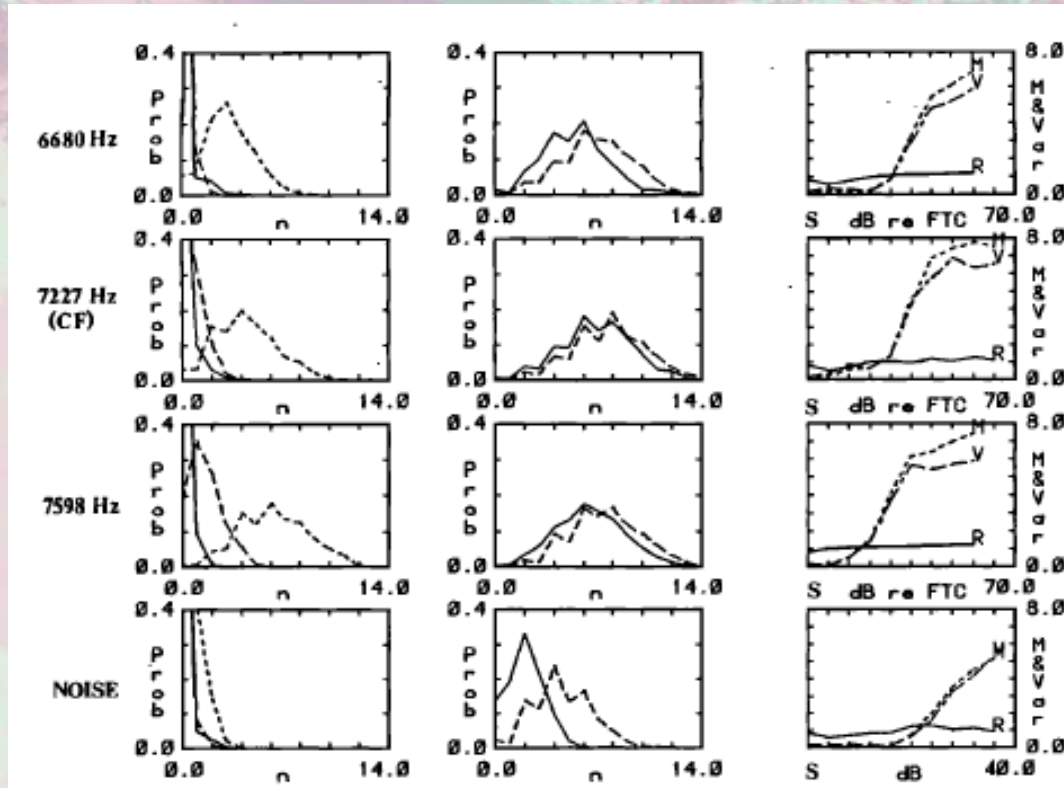
Malvin C. Teich and Shyam M. Khanna

Department of Electrical Engineering, Columbia University, New York, New York 10027 and Fowler Memorial Laboratory, Department of Otolaryngology, Columbia College of Physicians and Surgeons, New York, New York 10032



Khanna

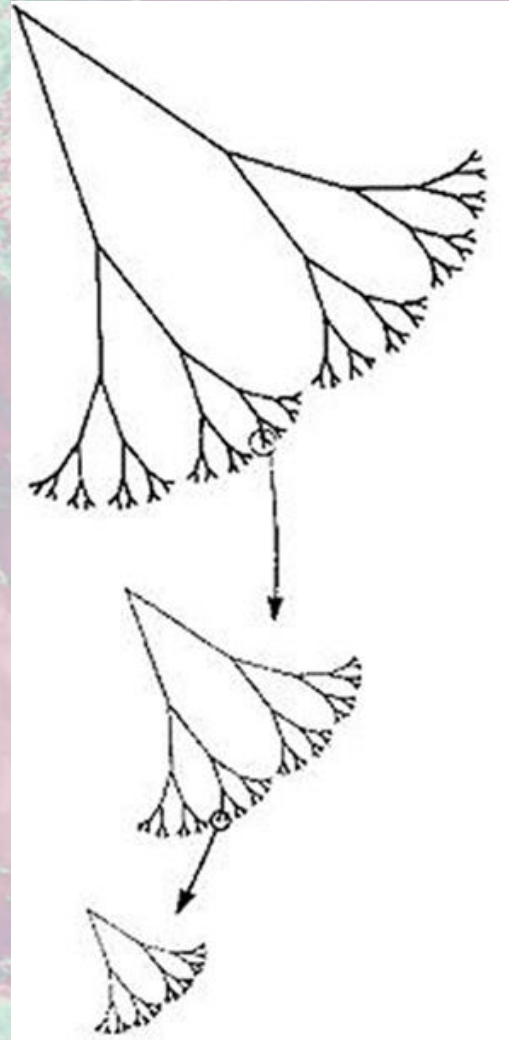
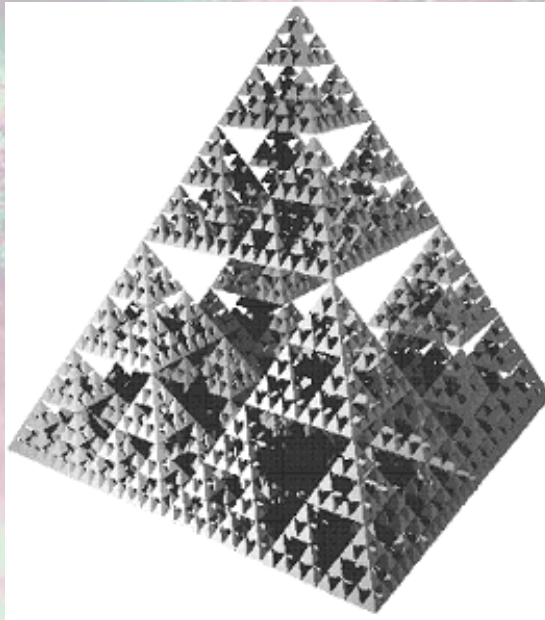
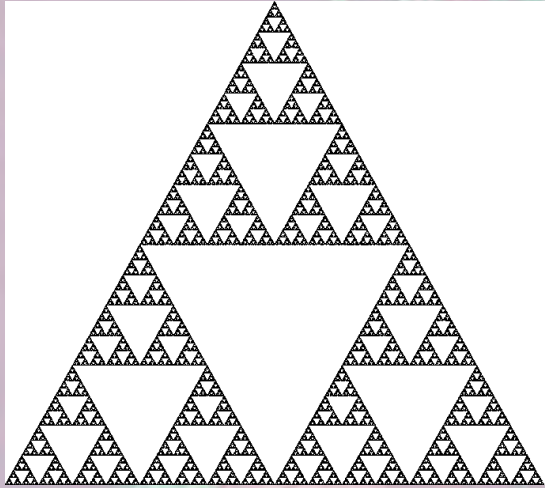
Eighth-nerve-fiber neural-counting experiments carried out at different sound-pressure levels using windows of $T = 50$ msec and $T = 200$ msec duration



SOME EVIDENCE OF EVENT PAIRS:

MIGHT A MULTINOMIAL MODEL REVEAL A HIDDEN NEURAL CODE? COE – March 4, 2009

3. FRACTALS AND FRACTAL POINT EVENTS



FORMS OF FRACTALS

- Deterministic
- Random
- Static
- Dynamical process

CUTOFFS

- Inner
- Outer

DEFINITIONS

- Scaling (both cutoffs)
- Fractal (no inner cutoff)
- Long-Range Dependence (no outer cutoff)

Mandelbrot



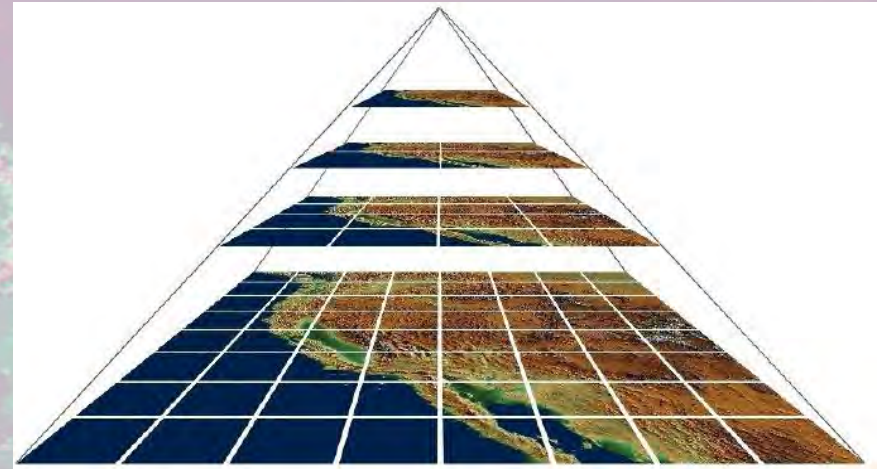
Adapted from B. B. Mandelbrot, *The Fractal Geometry of Nature* (Freeman, 1983).

VIEWING THE WORLD AT MULTIPLE SCALES

Volume:



Area:



Line:



Coastline Lengths at Different Scales:

MEASUREMENT SCALE (km)	MEASURED LENGTH (km)
0.694	534
6.94	314
69.4	133



Richardson

Penck (1894);

Richardson (1961):

$$d \propto s^c$$

The dependence of the measurement outcome on the scale chosen to make that measurement is the hallmark of a FRACTAL OBJECT

UBIQUITY OF FRACTAL BEHAVIOR

- Mathematics and physical sciences

- Fractal geometry of nature
- Noise in electronic components
- Fabricated nonperiodic layered structures
- Errors in telephone networks
- Photon statistics of Čerenkov radiation
- Earthquake patterns
- Computer network traffic

- Neurosciences

- Ion channels
- Membrane voltages
- Vesicular exocytosis and MEPCs
- Action-potential sequences
- Networks of cortical neurons
- Loudness and brightness functions
- Natural course of forgetting

- Medicine and human behavior

- Human standing and human gait
- Mood
- Human heartbeat patterns
- Movement patterns influenced by drugs

FRACTAL SHOT NOISE

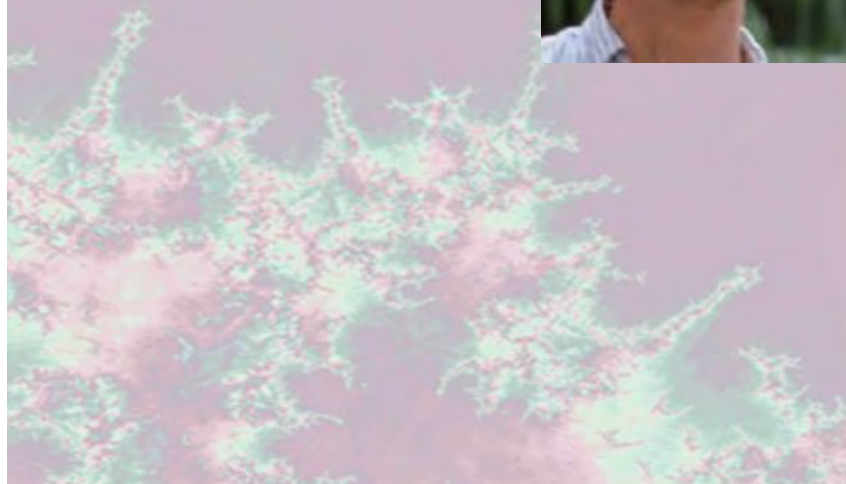
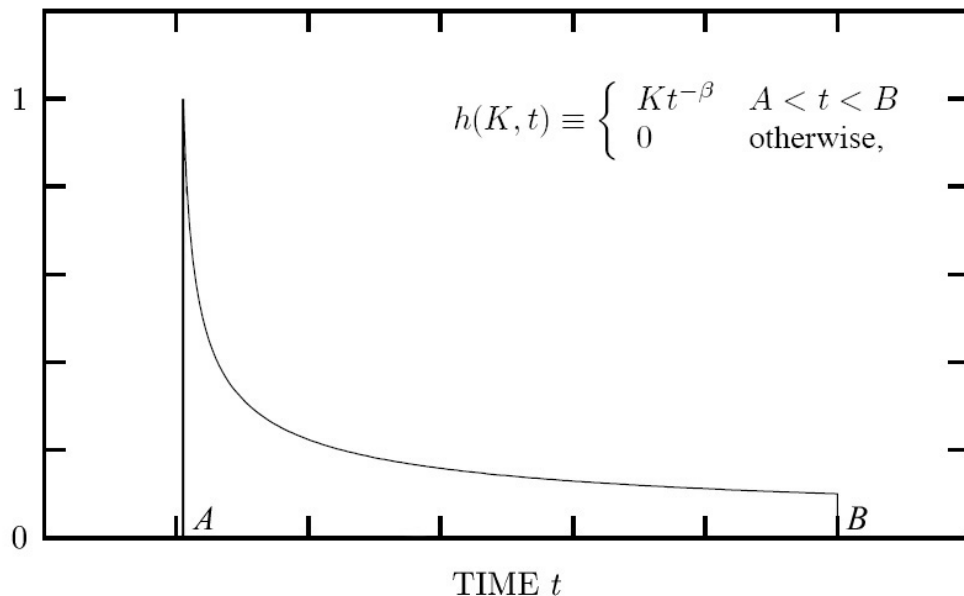
IEEE TRANSACTIONS ON INFORMATION THEORY, VOL. 36, NO. 6, NOVEMBER 1990

Power-Law Shot Noise

STEVEN B. LOWEN, STUDENT MEMBER, IEEE, AND MALVIN C. TEICH, FELLOW, IEEE



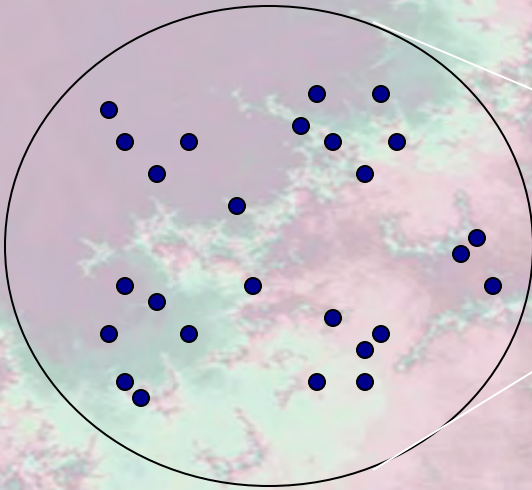
IMPULSE RESPONSE FUNCTION $h(t)$



$A > 0$ $B = \infty$	$A = 0$ $B = \infty$	$A = 0$ $B < \infty$	$A > 0$ $B < \infty$
-------------------------	-------------------------	-------------------------	-------------------------

$0 < \beta < \frac{1}{2}$ ($2 > \alpha > 1$)	$\Pr\{X = \infty\} = 1$ no $S(f)$	$E[X^2] = \infty$ $S \sim 1/f^\alpha$	$X \rightarrow \text{Gaussian}$ $S \sim 1/f^\alpha$	
$\frac{1}{2} \leq \beta < 1$ ($1 \geq \alpha > 0$)				
$\beta = 1$		$E[X] = \infty$ no $S(f)$	$X \rightarrow \text{Gaussian}$	
$\beta > 1$ ($0 < \zeta < 1$)	$X \rightarrow \text{Gaussian}$ $S(f)$ not $1/f^\alpha$	$X = \text{stable}$ no $S(f)$	$X \rightarrow \text{stable}$ no $S(f)$	$S(f)$ not $1/f^\alpha$

RANDOM POINT EVENTS IN SPACE AT MULTIPLE SCALES



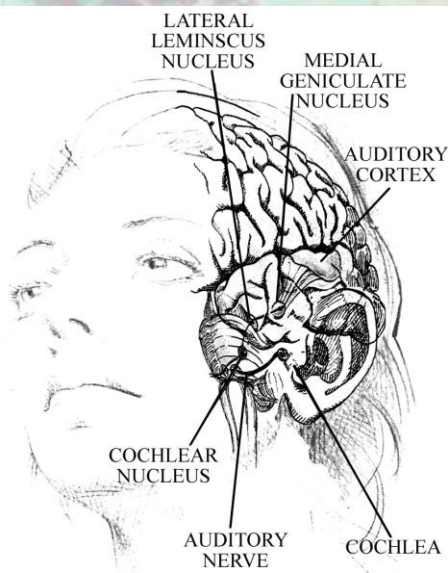
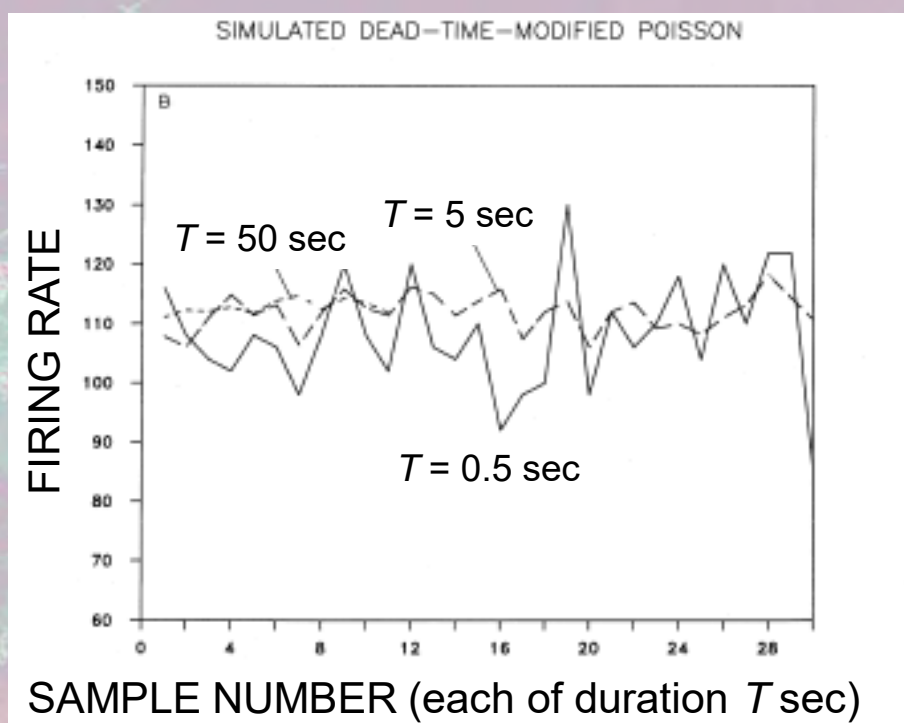
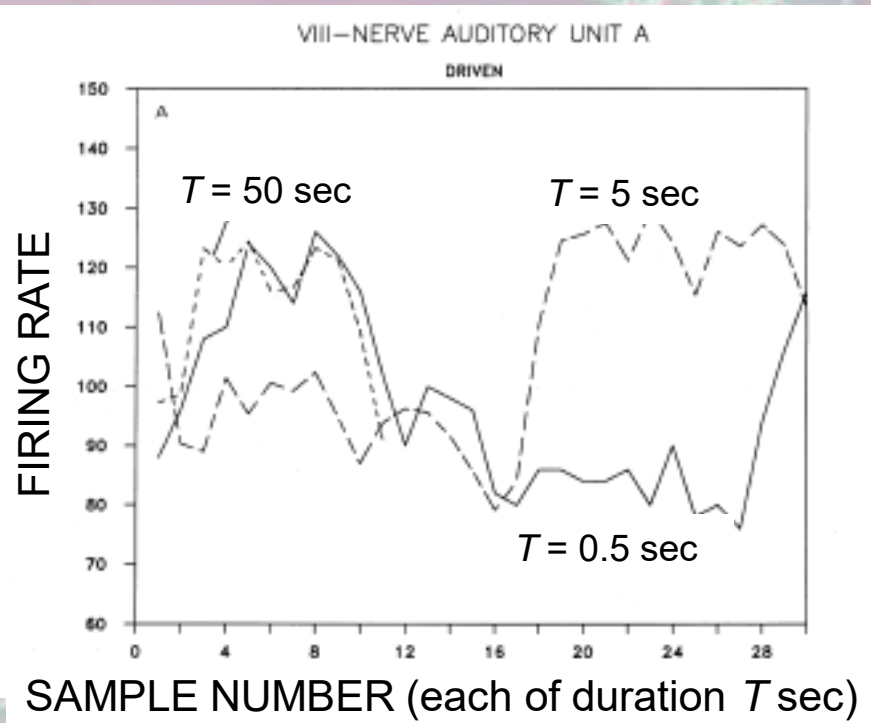
STARS, LIKE GALAXIES, TEND TO OCCUR IN CLUSTERS.

RANDOM POINT EVENTS IN TIME AT MULTIPLE SCALES



HOW DO THE RATE FLUCTUATIONS OF A SEQUENCE OF RANDOM POINT EVENTS BEHAVE AS THE COUNTING WINDOW DURATION INCREASES?

RATE FLUCTUATIONS IN AN AUDITORY NERVE FIBER



SNR_{λ} is observed to be essentially independent of T (counting window duration)

For Poisson: $\text{var}(n) \equiv \sigma_n^2 = \bar{n}$

$SNR = \bar{n} / \sigma_n = \sqrt{\bar{n}}$

Rate $\lambda \equiv n/T$ so $\bar{\lambda} = \bar{n}/T$ and $\sigma_{\lambda} = \sigma_n/T$

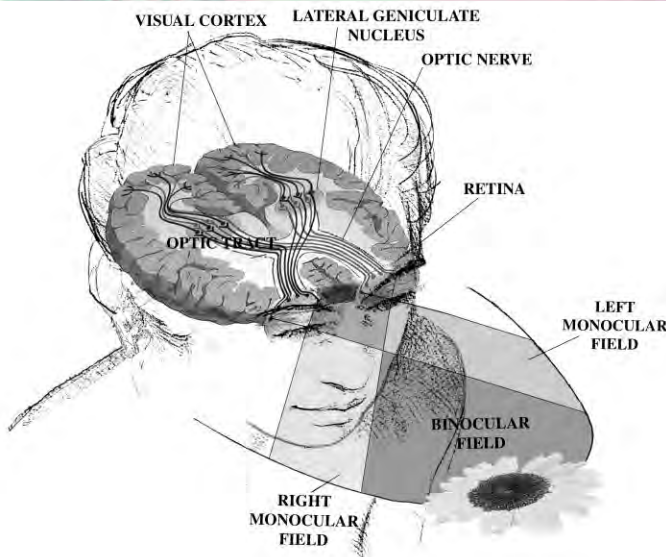
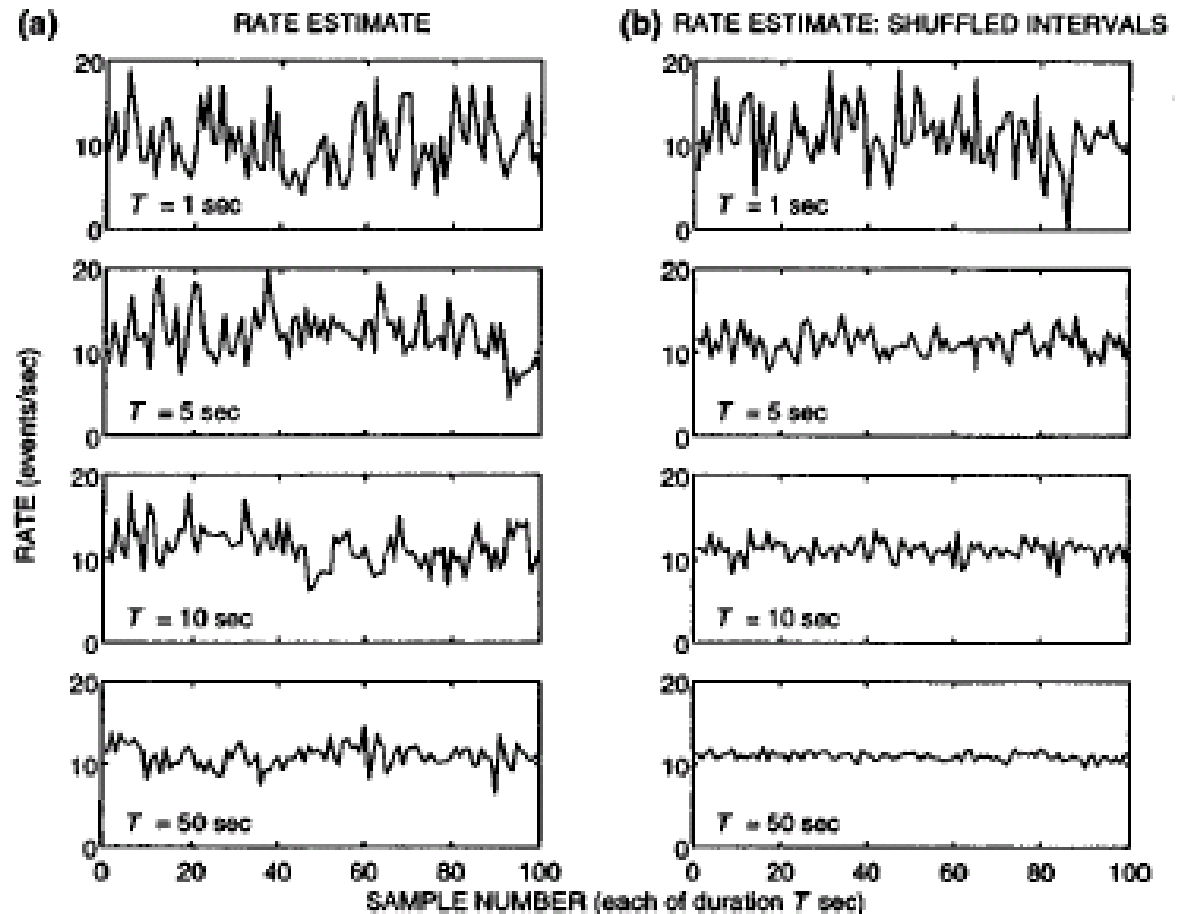
Thus, $SNR_{\lambda} \equiv \bar{\lambda} / \sigma_{\lambda} = SNR_n \propto T^{1/2}$

Hence, $SNR_{\lambda} \uparrow$ as $T \uparrow$

After Teich, "Fractal Character of the Auditory Neural Spike Train," *IEEE Trans. Biomed. Eng.* **36**, 150-160 (1989); and Teich, Johnson, Kumar, and Turcott, "Rate Fluctuations and Fractional Power-Law Noise Recorded from Cells in the Lower Auditory Pathway of the Cat," *Hearing Res.* **46**, 41-52 (1990).

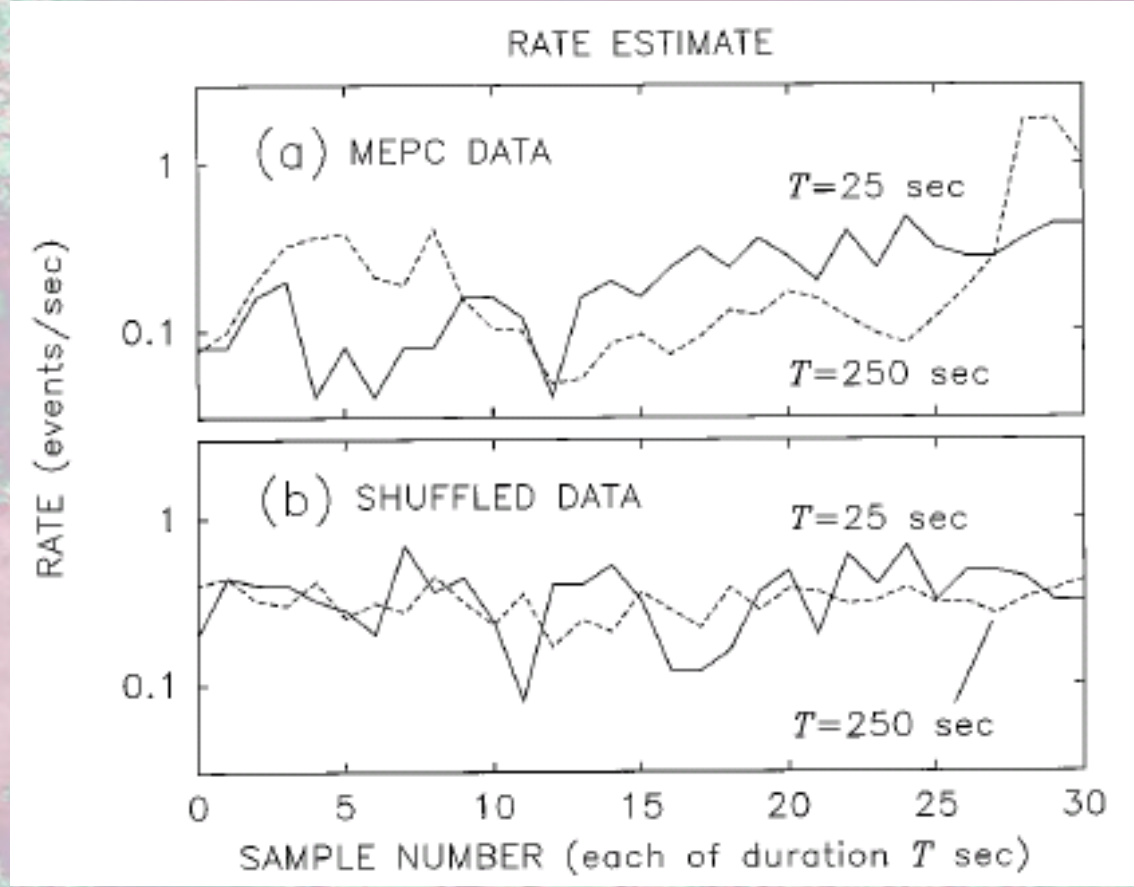
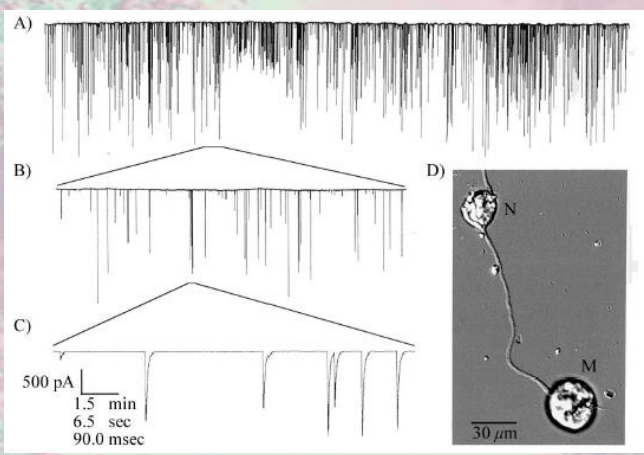
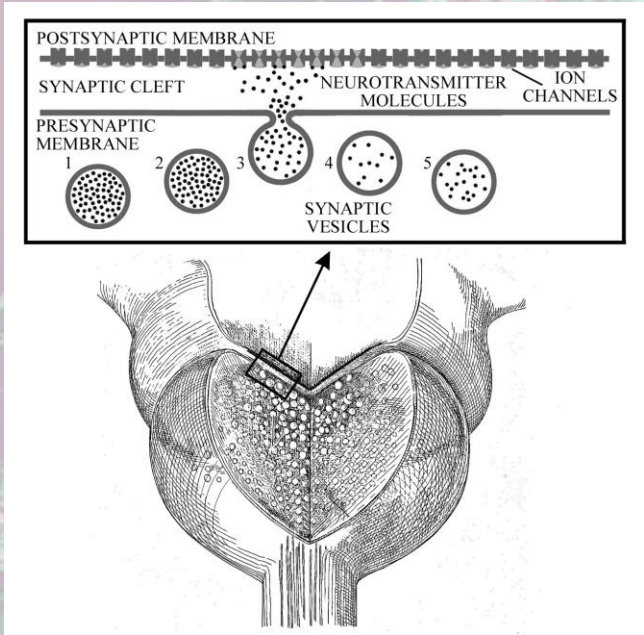
RATE FLUCTUATIONS IN A VISUAL-SYSTEM NERVE FIBER (RGC MAINTAINED DISCHARGE)

SNR_{λ} increases with T , but far more slowly than for the shuffled intervals (Poisson data)



After Teich, Heneghan, Lowen, Ozaki, and Kaplan, "Fractal Character of the Neural Spike Train in the Visual System of the Cat," *J. Opt. Soc. Am. A* 14, 529-546 (1997).

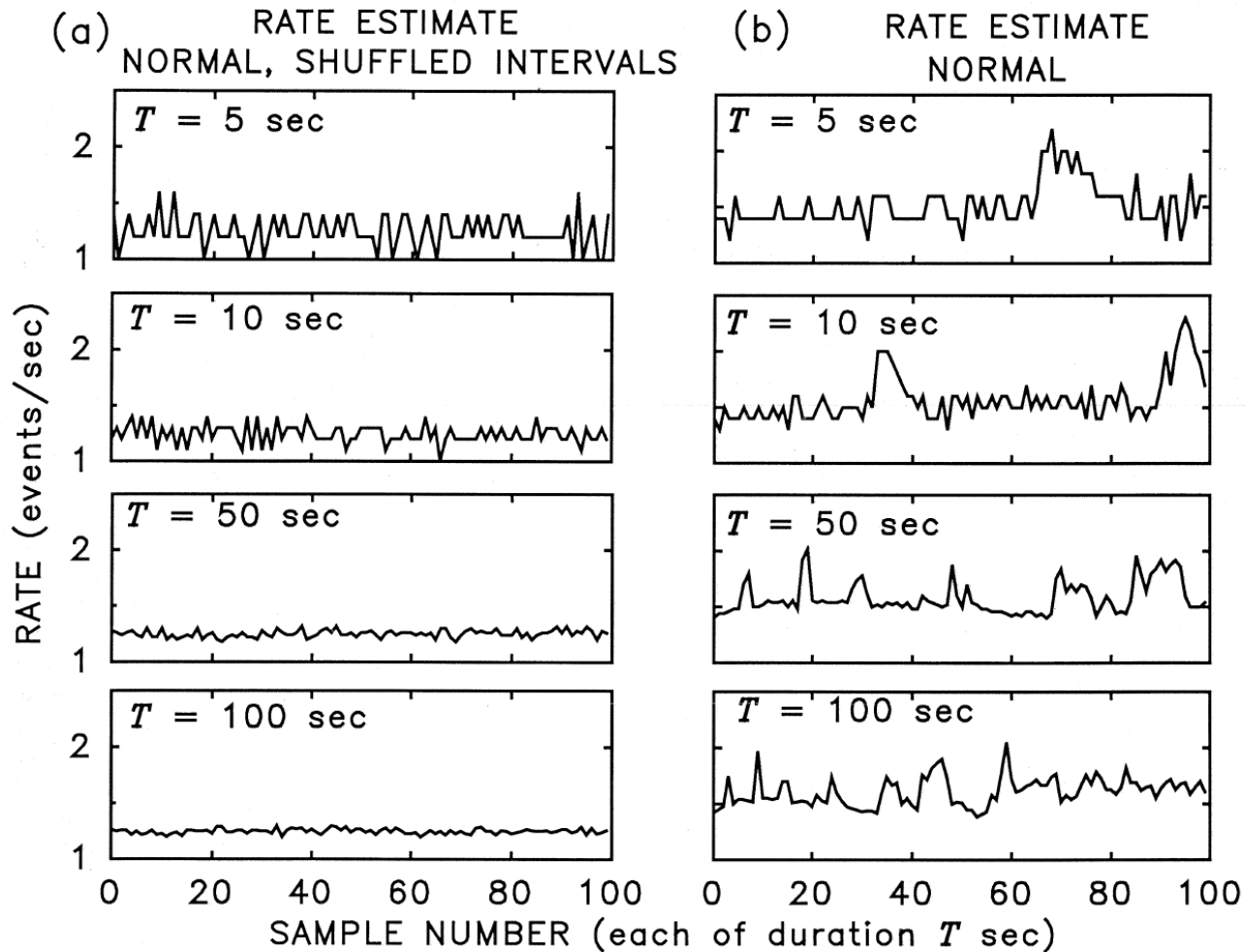
RATE FLUCTUATIONS OF VESICULAR NEUROTRANSMITTER EXOCYTOSIS AT *XENOPUS* NEUROMUSCULAR JUNCTION



SNR_{λ} is essentially independent of T for the miniature end-plate current (MEPC) data

After Lowen, Cash, Poo, and Teich, "Quantal Neurotransmitter Secretion Rate Exhibits Fractal Behavior," *J. Neurosci.* 17, 5666-5677 (1997).

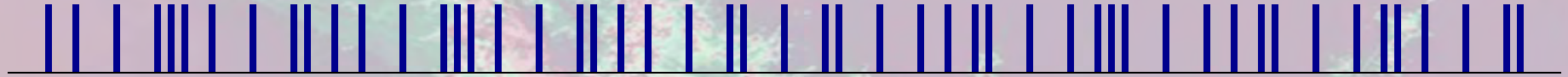
RATE FLUCTUATIONS IN THE HUMAN HEARTBEAT



SNR_λ is nearly independent of T for the human heart rate

After Turcott and Teich, "Fractal Character of the Electrocardiogram: Distinguishing Heart-Failure and Normal Patients," *Ann. Biomed. Eng.* **24**, 269-293 (1996).

COUNTING POINT EVENTS IN A DIFFERENTIATING TIME WINDOW [NORMALIZED HAAR-WAVELET VARIANCE $A(T)$]

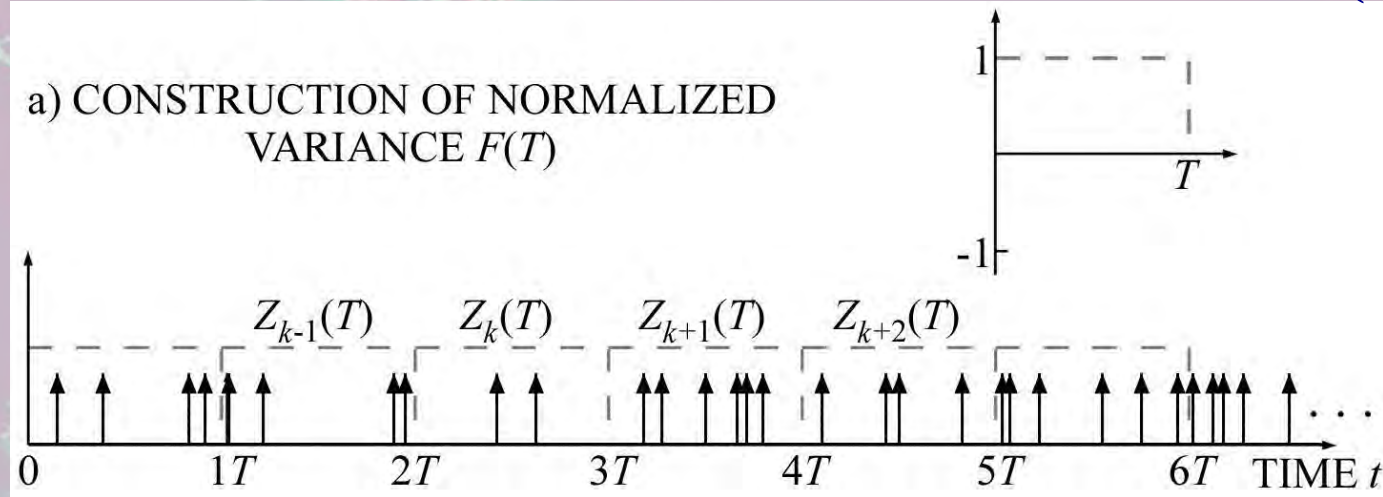


Random point events in time often exhibit self-scaling that takes the form of power-law behavior in their statistics (e.g., spectrum and count variance-to-mean ratio):

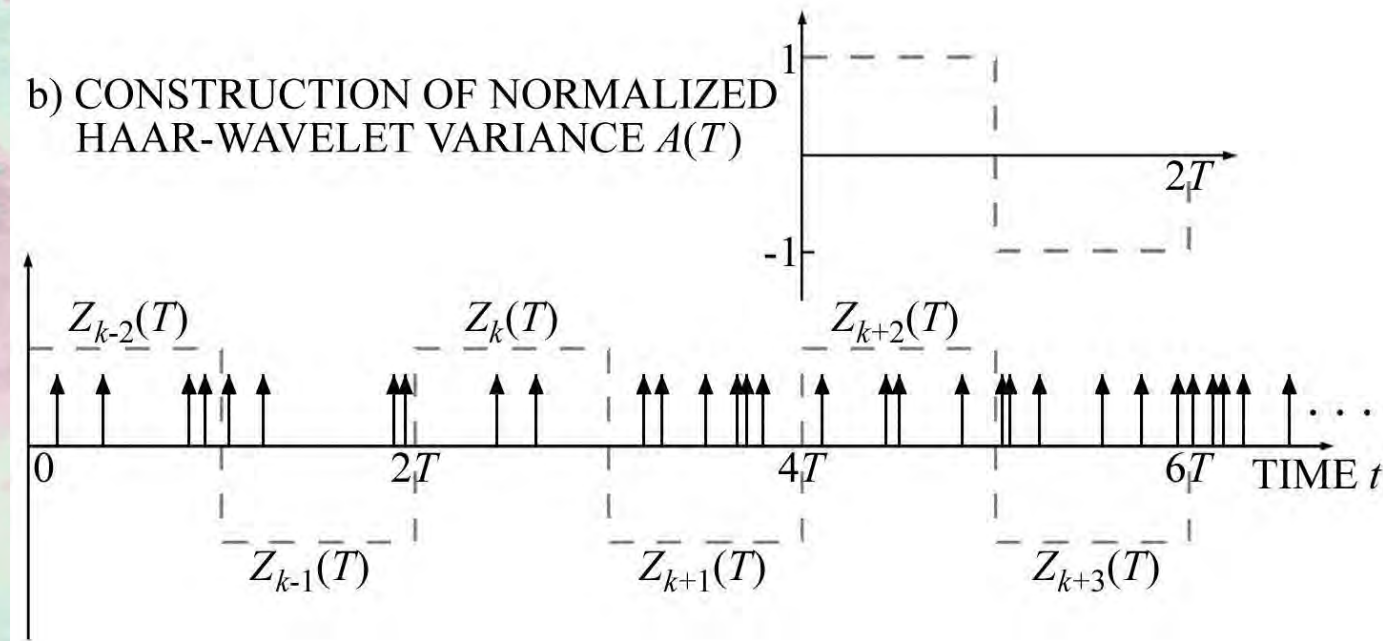
FRACTAL BEHAVIOR OF POINT EVENTS

NORMALIZED VARIANCE $F(T)$ AND NORMALIZED HAAR-WAVELET VARIANCE $A(T)$

a) CONSTRUCTION OF NORMALIZED VARIANCE $F(T)$



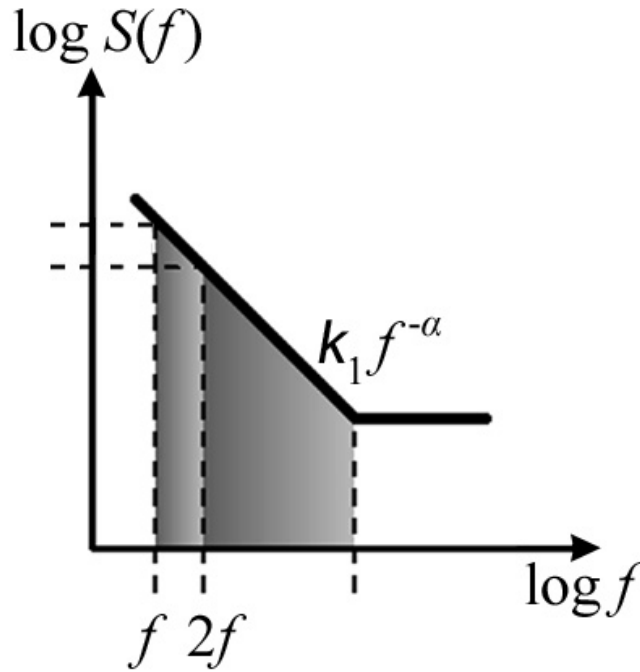
b) CONSTRUCTION OF NORMALIZED HAAR-WAVELET VARIANCE $A(T)$



POWER-LAW SCALE INVARIANCE



Pareto

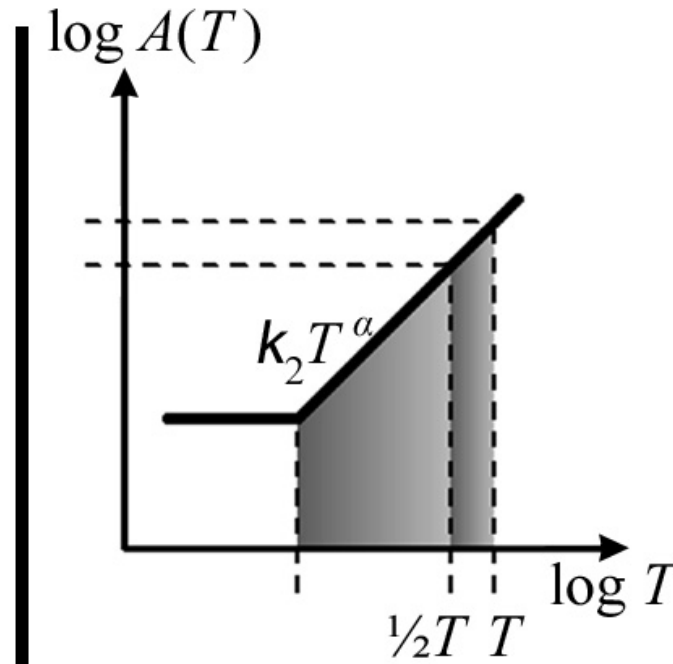


$$\frac{S(f)}{S(2f)} = \frac{k_1 f^{-\alpha}}{k_1 (2f)^{-\alpha}} = 2^\alpha$$

INDEPENDENT OF f



SCALE INVARIANT



$$\frac{A(T)}{A(T/2)} = \frac{k_2 T^\alpha}{k_2 (T/2)^\alpha} = 2^\alpha$$

INDEPENDENT OF T



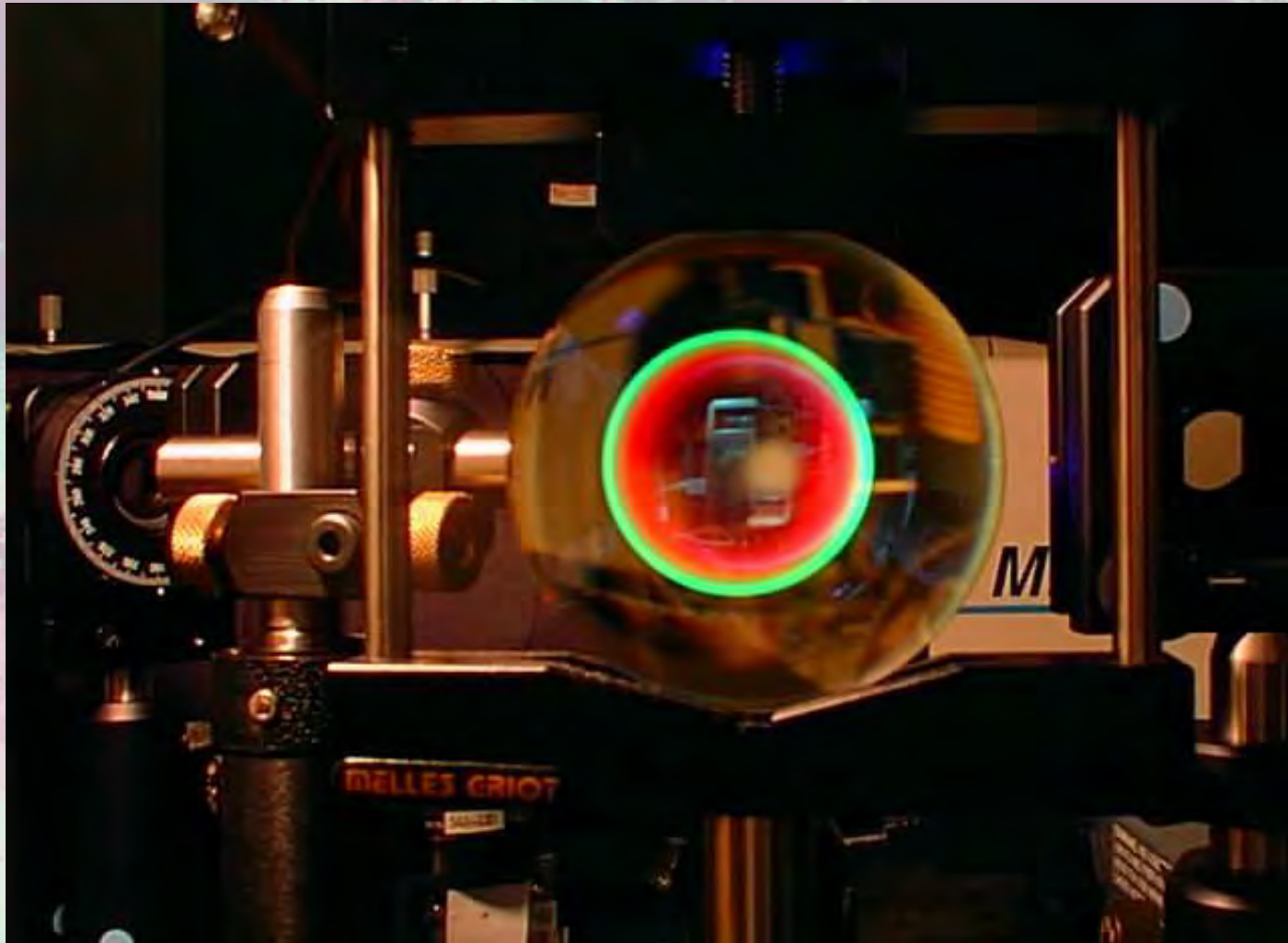
SCALE INVARIANT

α = SCALING EXPONENT

■ = SCALING RANGE

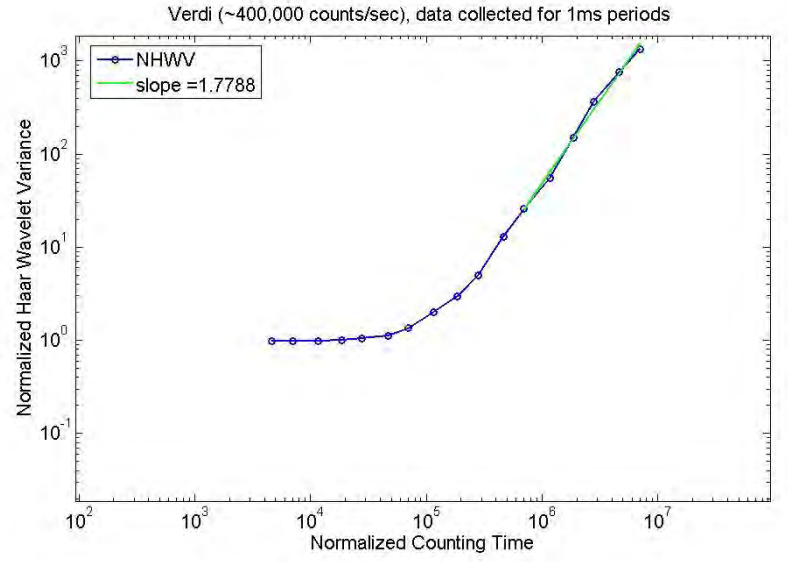
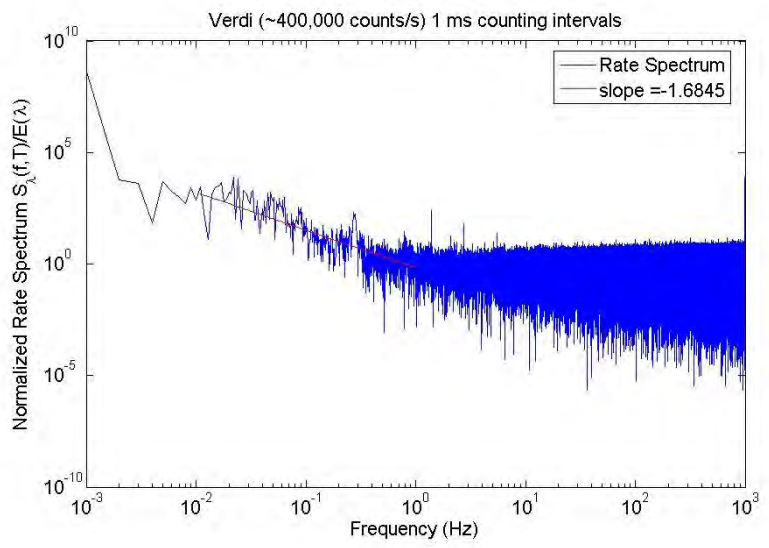
4. FRACTAL PHOTONS

**BU PHOTONICS CENTER
QUANTUM PHOTONICS LAB – ROOM 733**



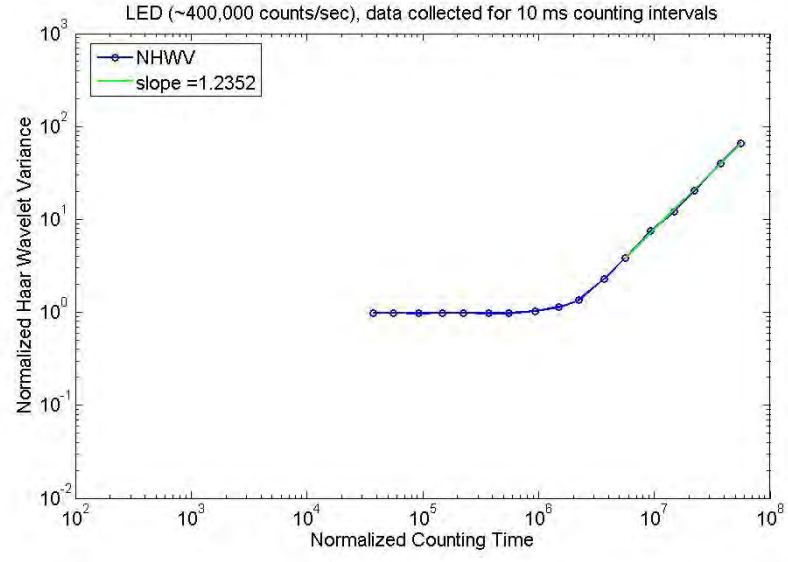
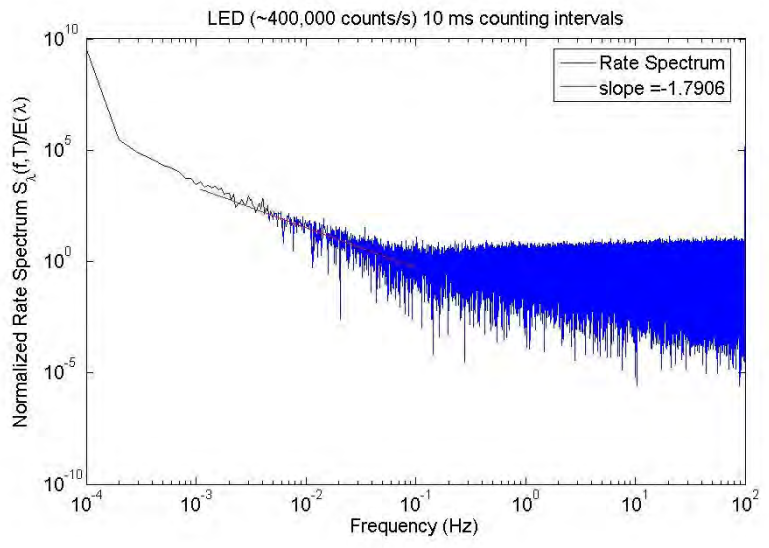
LASER

FREQUENCY-DOUBLED Nd³⁺:YVO₄ LASER OPERATING AT 532 nm



LED

COMMERCIAL BLUE LED WITH CENTRAL WAVELENGTH OF 430 nm



ORIGINS OF FRACTAL BEHAVIOR

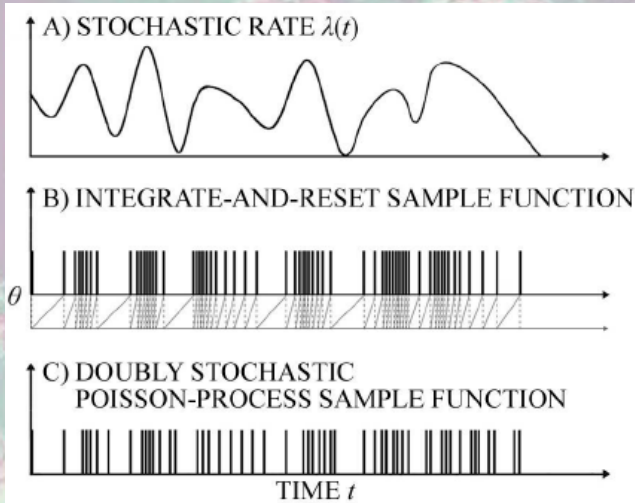
- Empirical power-law behavior
- Diffusion
- Convergence to stable (Lévy) distributions
- Lognormal distribution
- Self-organized criticality
- Highly optimized tolerance
- Scale-free networks
- Superposition of relaxation processes

FRactal-Based POINT-PROCESSES – MODELS

Fractal Gaussian Noise



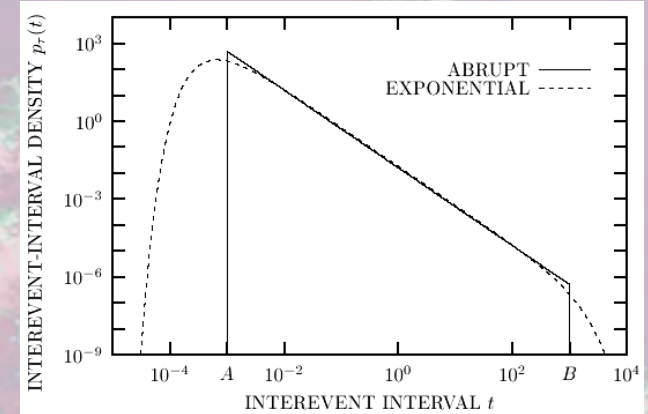
Kolmogorov



Fractal Renewal Process



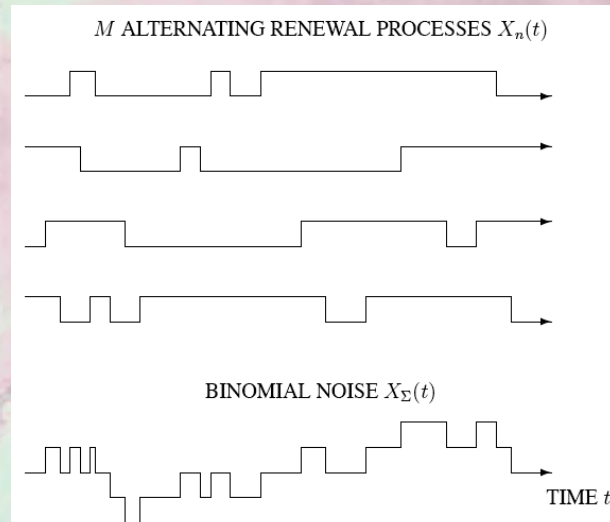
Mandelbrot



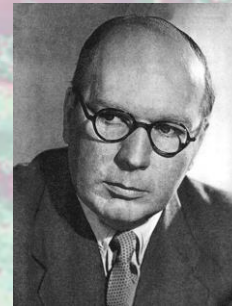
Alternating Fractal Renewal Process



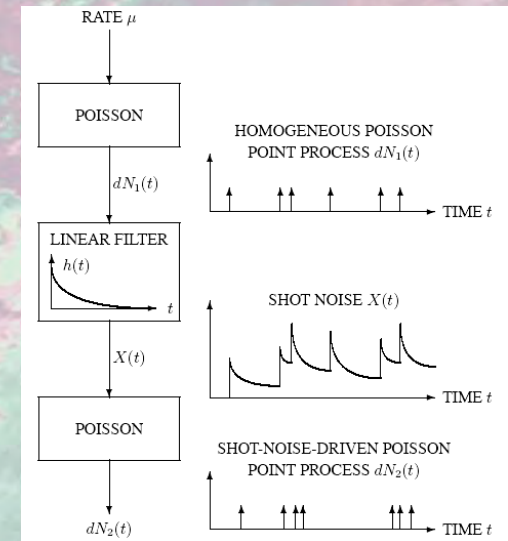
Gauss



Fractal Shot-Noise-Driven Poisson



Bartlett

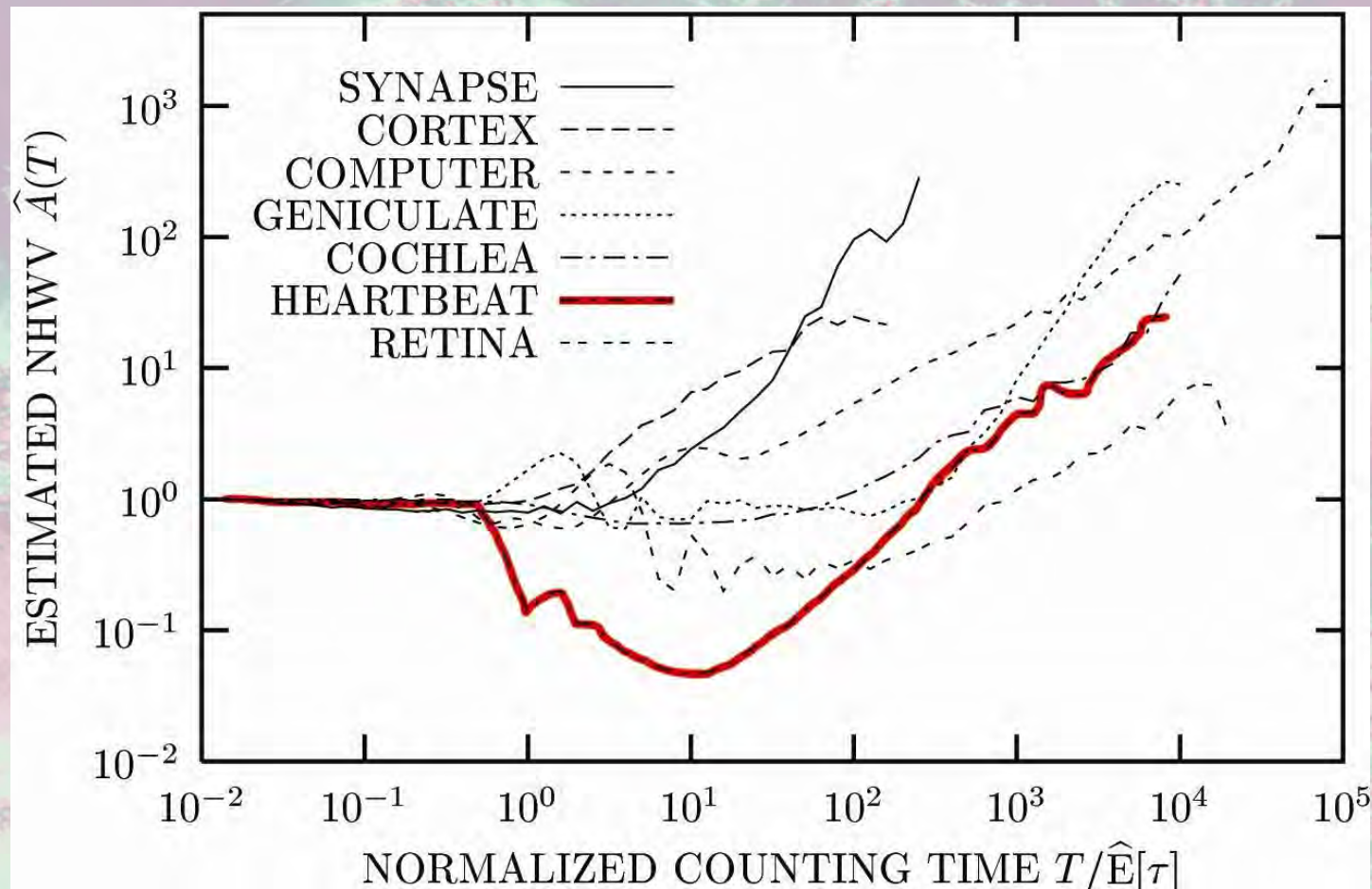


5. HEART RATE VARIABILITY

CAN BE STUDIED VIA:

COUNTS -- Duration of time window selected by experimenter affects observation or

TIME INTERVALS: More exhaustive since all information is retained



CONGESTIVE HEART FAILURE

INABILITY OF HEART TO INCREASE CARDIAC OUTPUT IN PROPORTION TO METABOLIC DEMANDS

Symptom complex:

Many different presentations and etiologies

Typical symptoms:

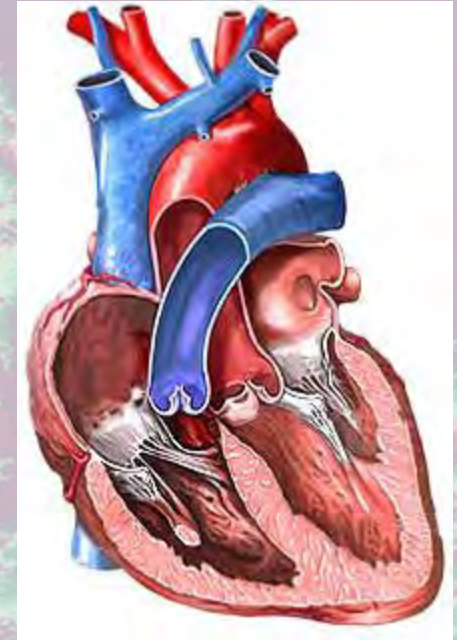
- Shortness of breath
- Swelling in legs
- General fatigue and weakness

Clinical diagnostics:

- Ascultate heart
- Carotid pulse
- Electrocardiogram
- Chest radiograph

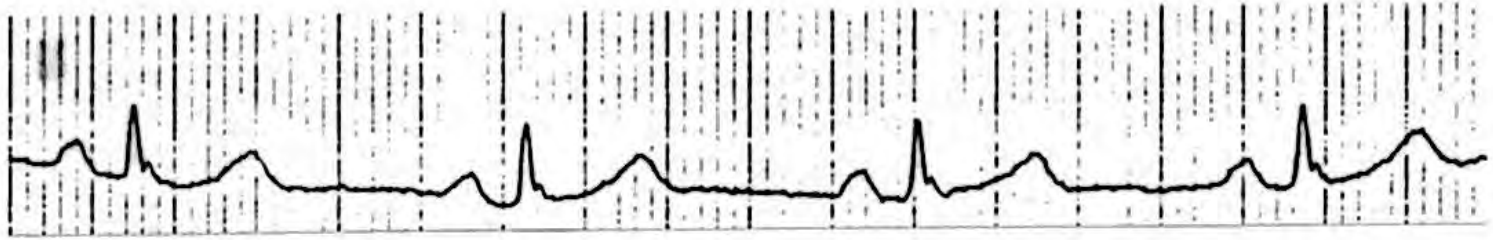
Collaborators:

- **Steven Lowen, Harvard Medical School**
- **Conor Heneghan, University College Dublin**
- **Robert Turcott, Stanford Medical School**
- **Markus Feurstein, Wirtschaftsuniversität Wien**
- **Stefan Thurner, Allgemeines Krankenhaus Wien**

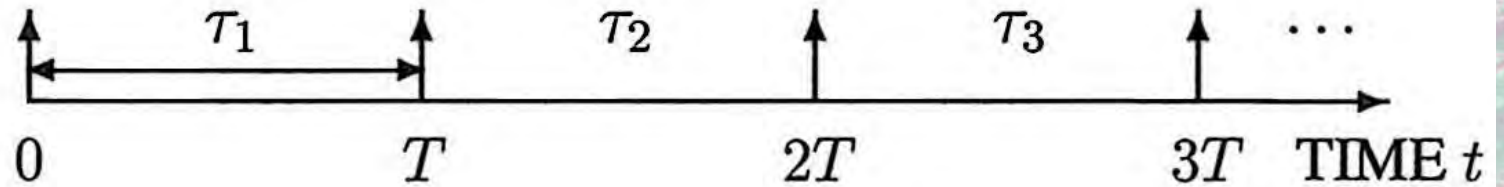


ELECTROCARDIOGRAM

a)



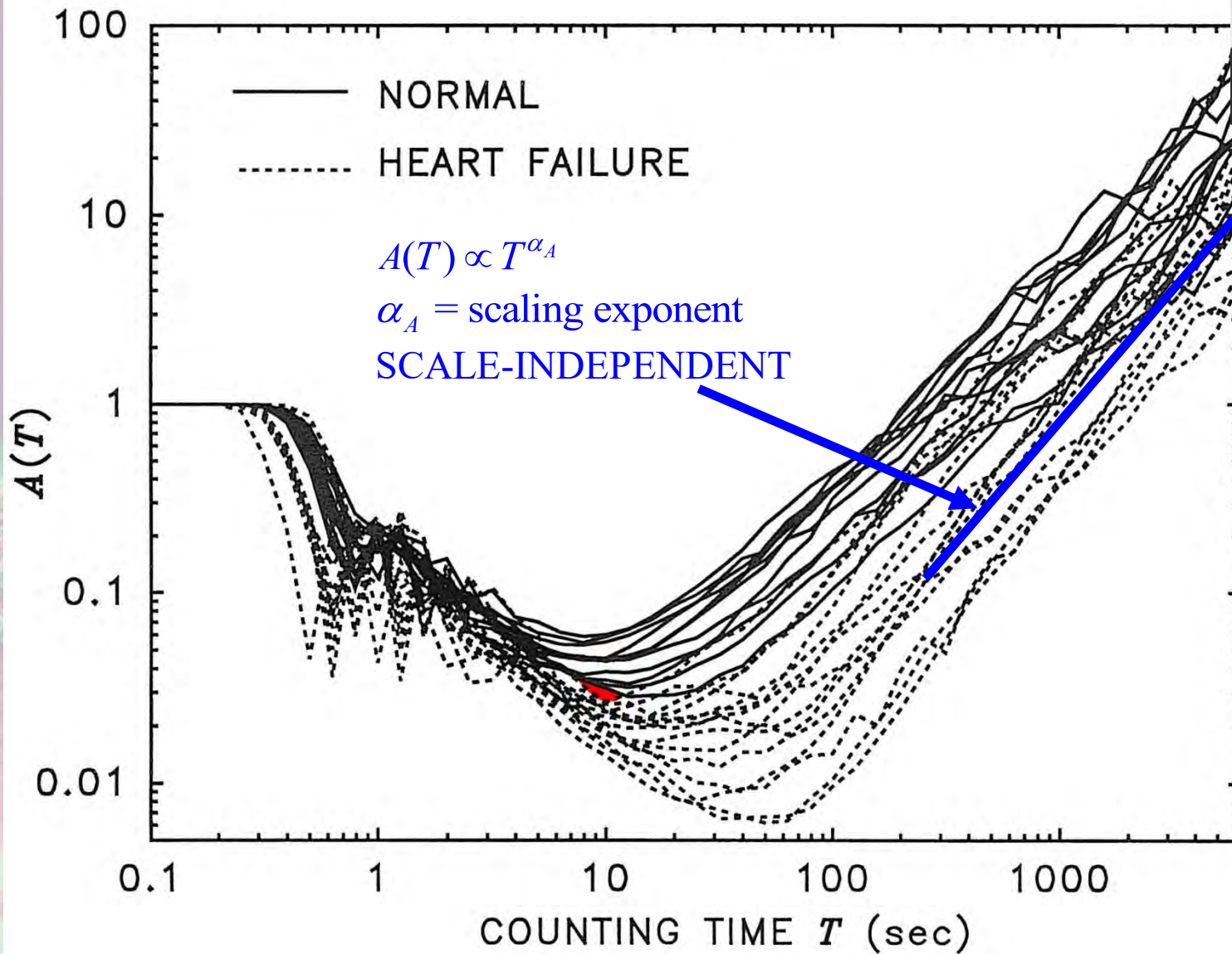
b)



NORMALIZED HAAR-WAVELET VARIANCE



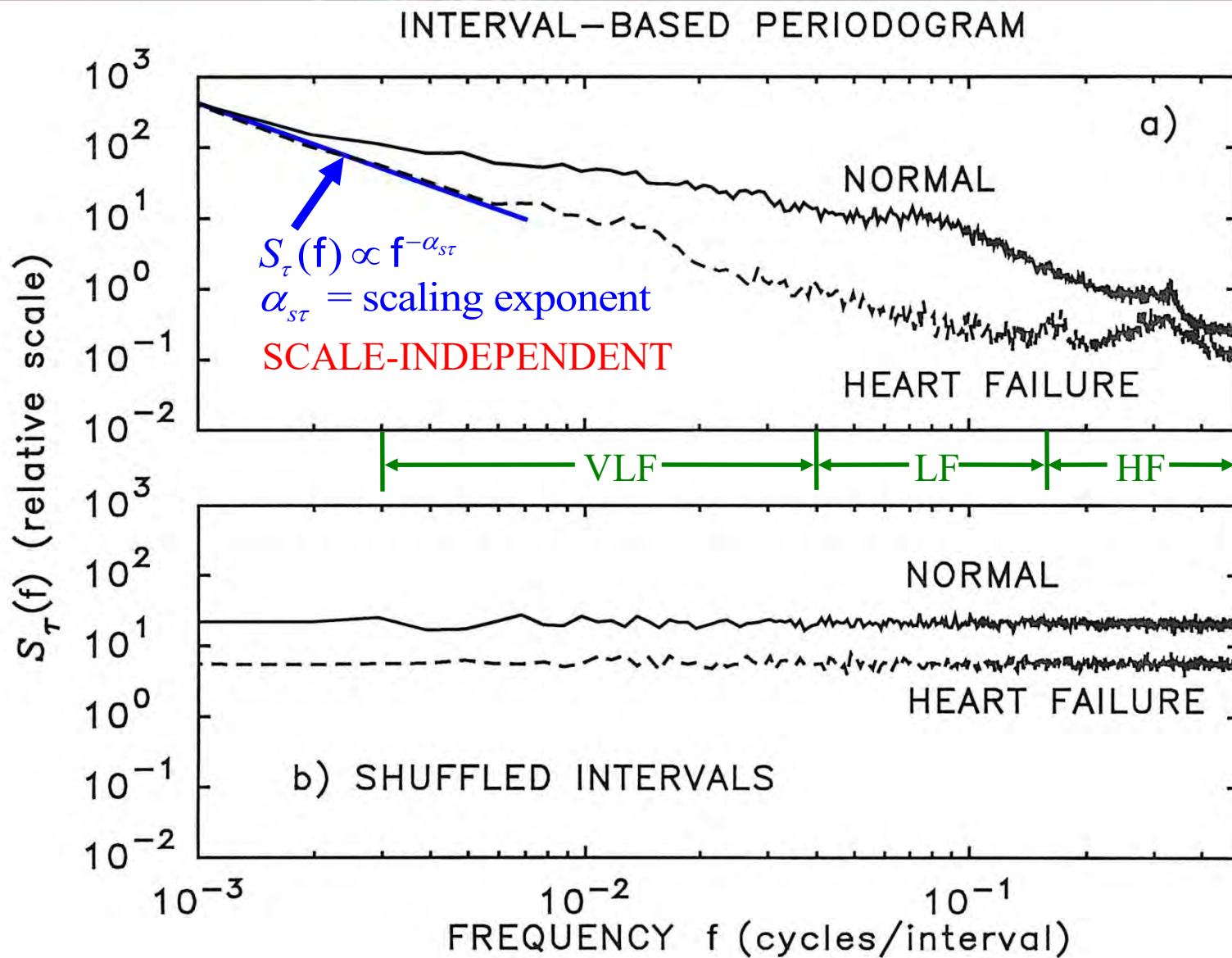
Allan



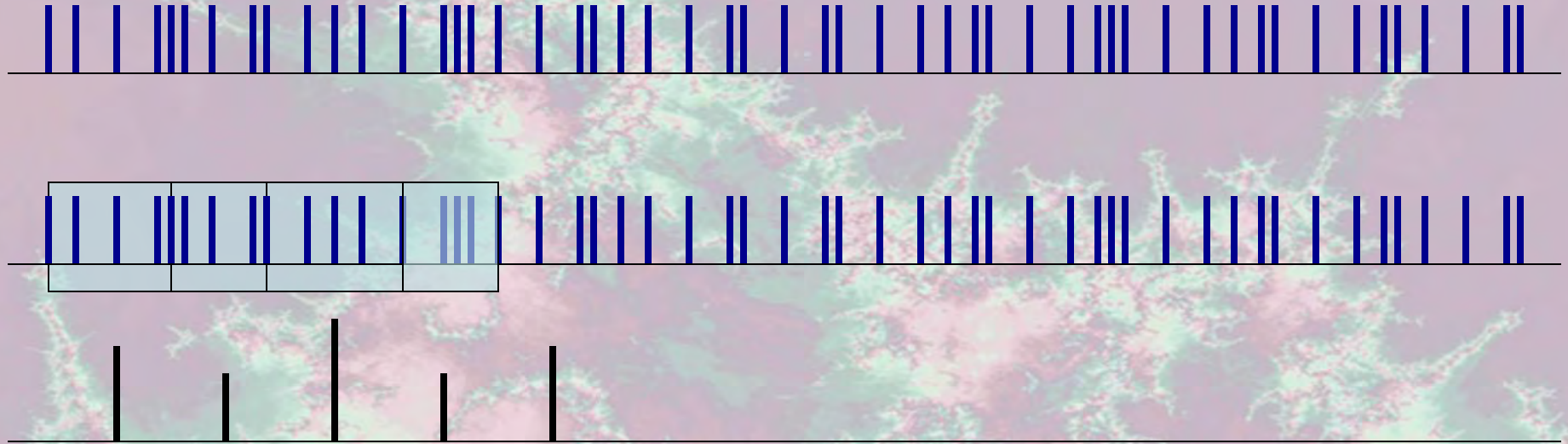
INTERVAL-BASED MEASURES: SPECTRUM



Fourier



INTERVAL-BASED HAAR WAVELET





INTERVAL-BASED TIME-SCALE ANALYSIS

DISCRETE WAVELET TRANSFORM

EXAMINES ALL SCALES

MITIGATES AGAINST NONSTATIONARITIES

m = scale index; 2^m = scale

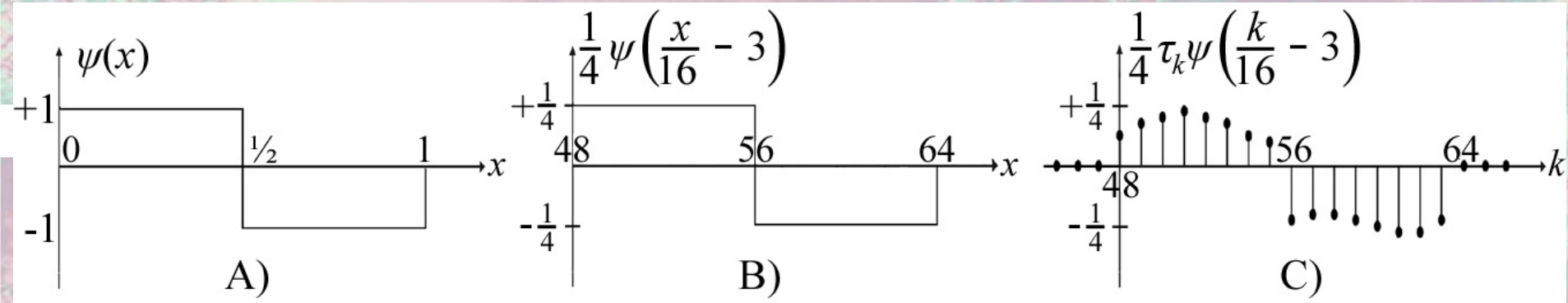


Haar

$$W_{\psi, \tau}^{\text{wav}}(m, i) = \sum_k 2^{-m/2} \psi(2^{-m}k - i) \tau_k$$

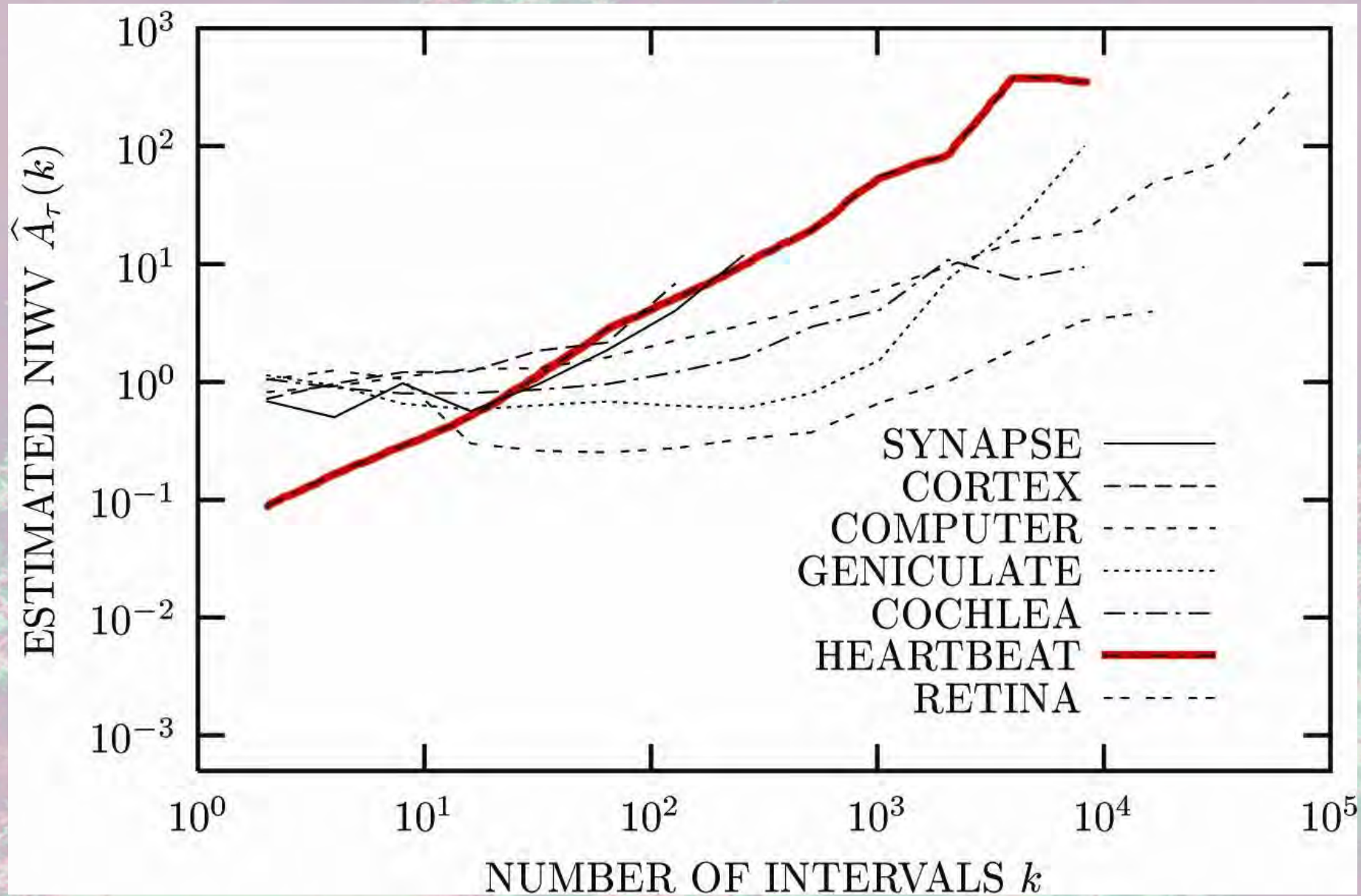
$$\sigma_{\text{wav}}^2 \equiv \text{Var} \left[W_{\psi, \tau}^{\text{wav}}(m, i) \right] = 2^{-m} \sum_k \sum_l \psi(2^{-m}k - i) \psi(2^{-m}l - i) R_{\tau}(l - k)$$

$$A_{\tau}(k) \equiv \text{Var} \left[W_{\psi, \tau}^{\text{wav}}(m, i) \right] / \text{Var} [\tau]$$

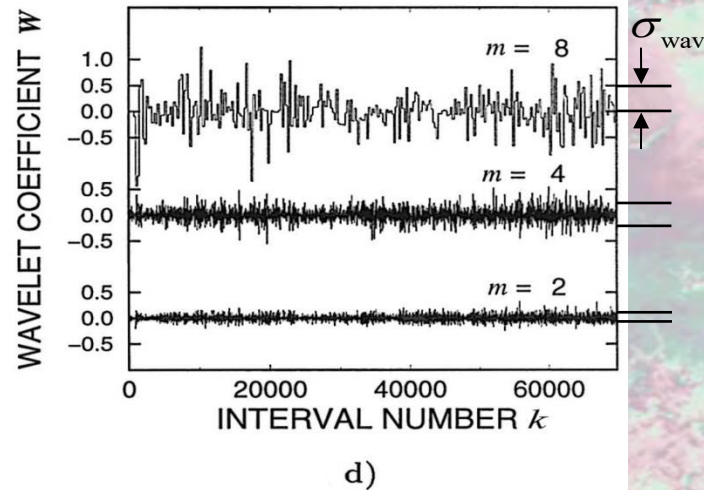
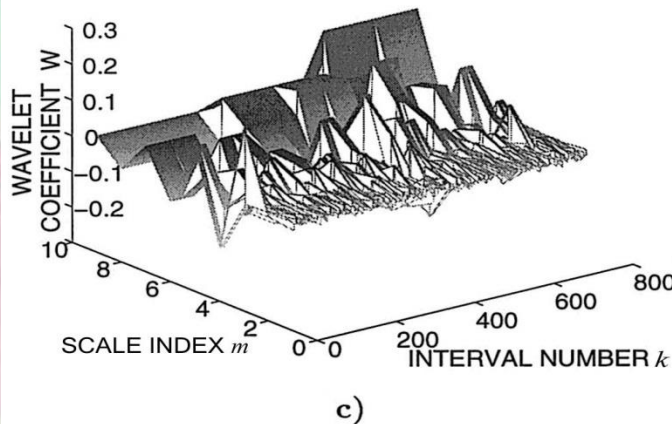
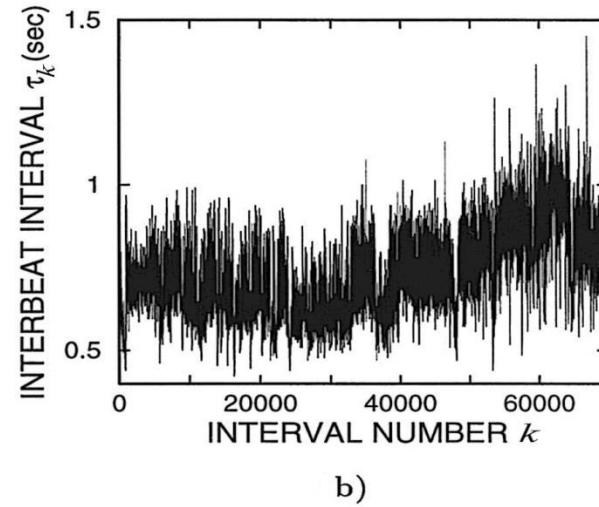
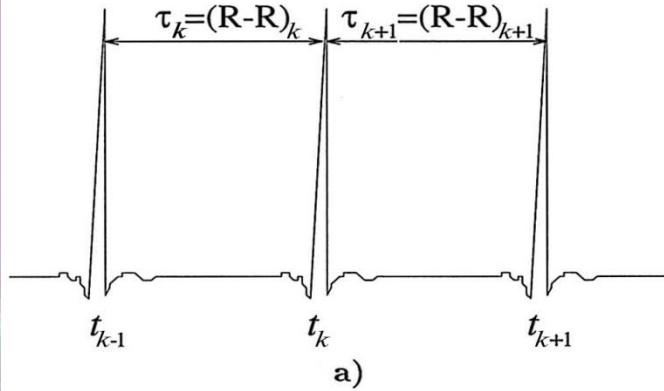


After Teich, Lowen, Jost, Vibe-Rheymer, and Heneghan, "Heart-Rate Variability: Measures and Models," in *Nonlinear Biomedical Signal Processing, Vol. II, Dynamic Analysis and Modeling*, edited by M. Akay (IEEE Press, New York, 2001), ch. 6, pp. 159-213.

INTERVAL-BASED MEASURES: NIWV

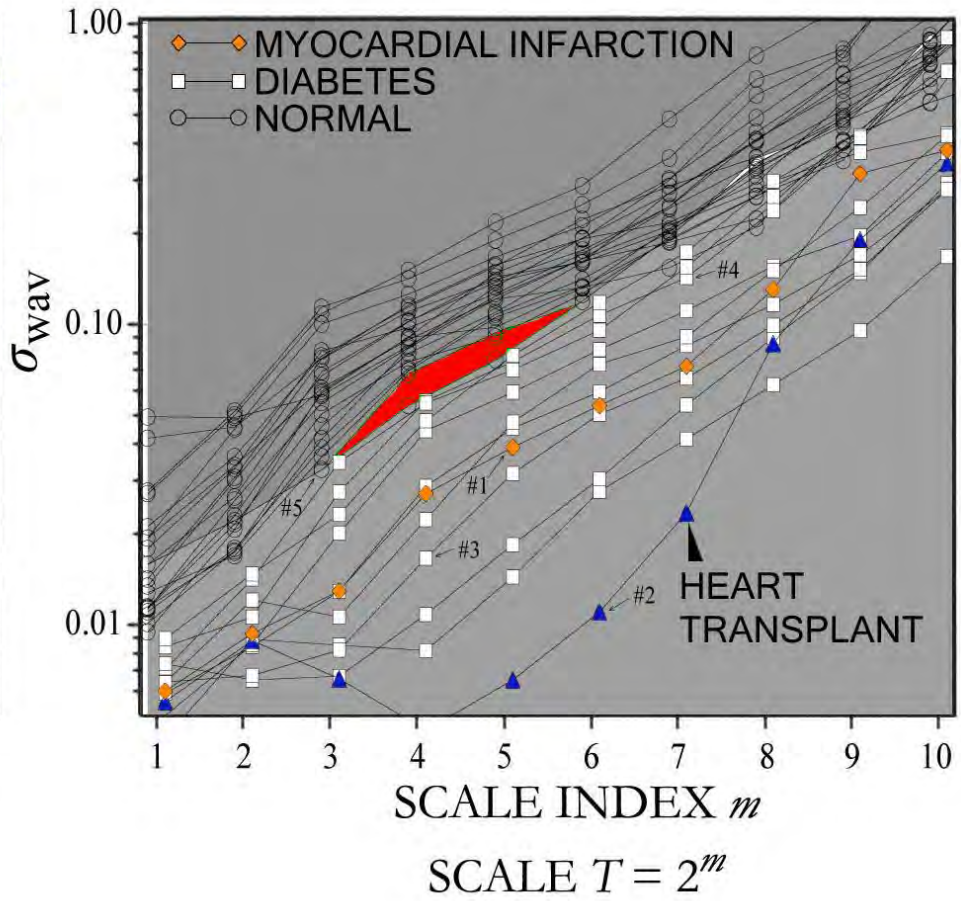
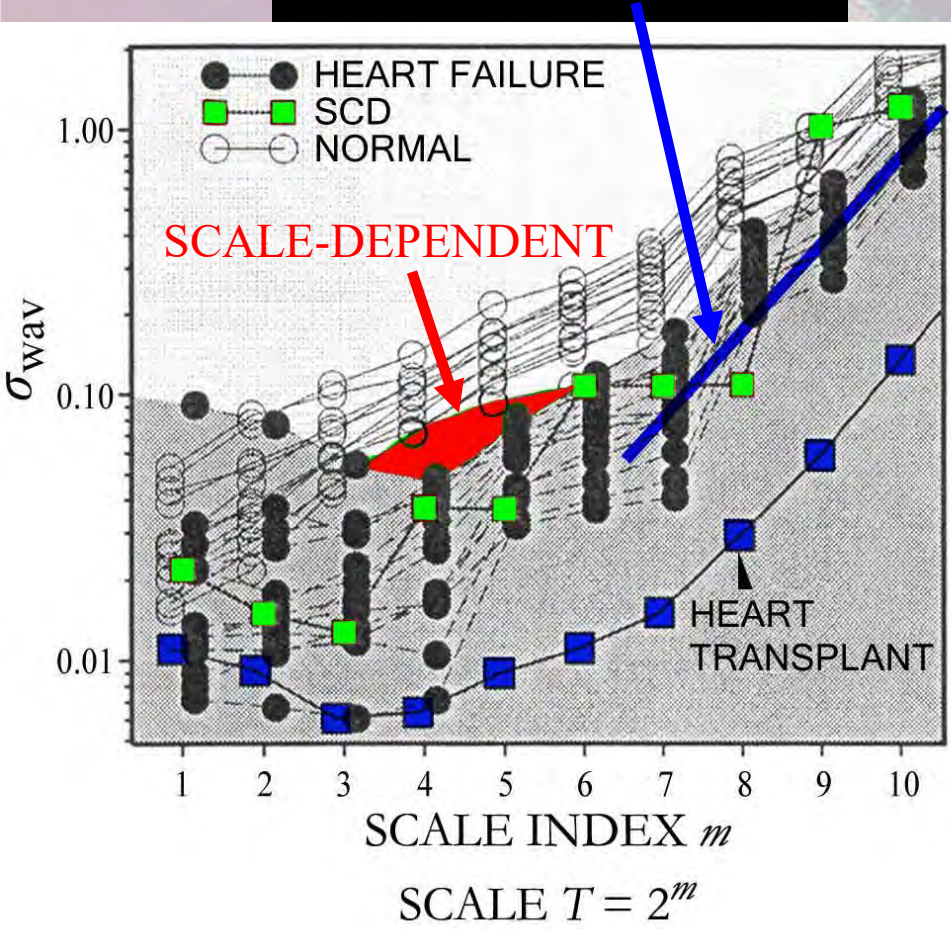


NORMAL



After Teich, Lowen, Jost, Vibe-Rheymer, and Heneghan, "Heart-Rate Variability: Measures and Models," in *Nonlinear Biomedical Signal Processing, Vol. II, Dynamic Analysis and Modeling*, edited by M. Akay (IEEE Press, New York, 2001), ch. 6, pp. 159-213.

$\sigma_{\text{wav}}^2(T) \propto T^{\alpha_{Ar}}$
 α_{Ar} = scaling exponent
SCALE-INDEPENDENT



After Teich, *Proc. Int. Conf. IEEE Eng. Med. Biol. Soc.* **20**, 1136-1141 (1998).

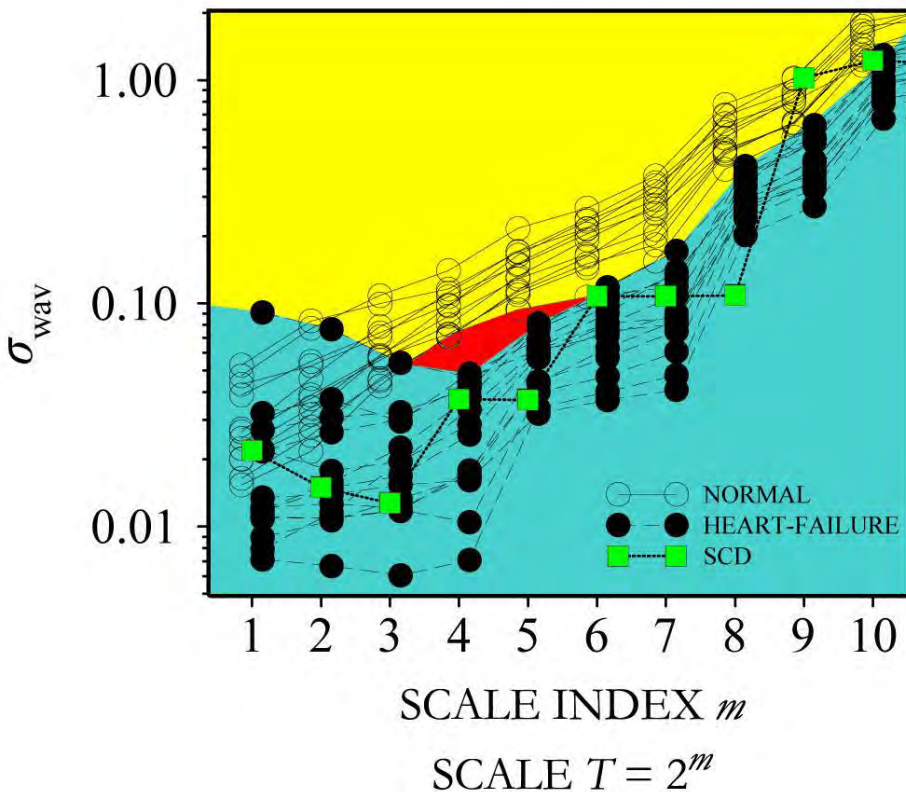
After Ashkenazy et al., *Fractals* **6**, 197-203 (1998).

ROBUSTNESS WITH FORM OF WAVELET

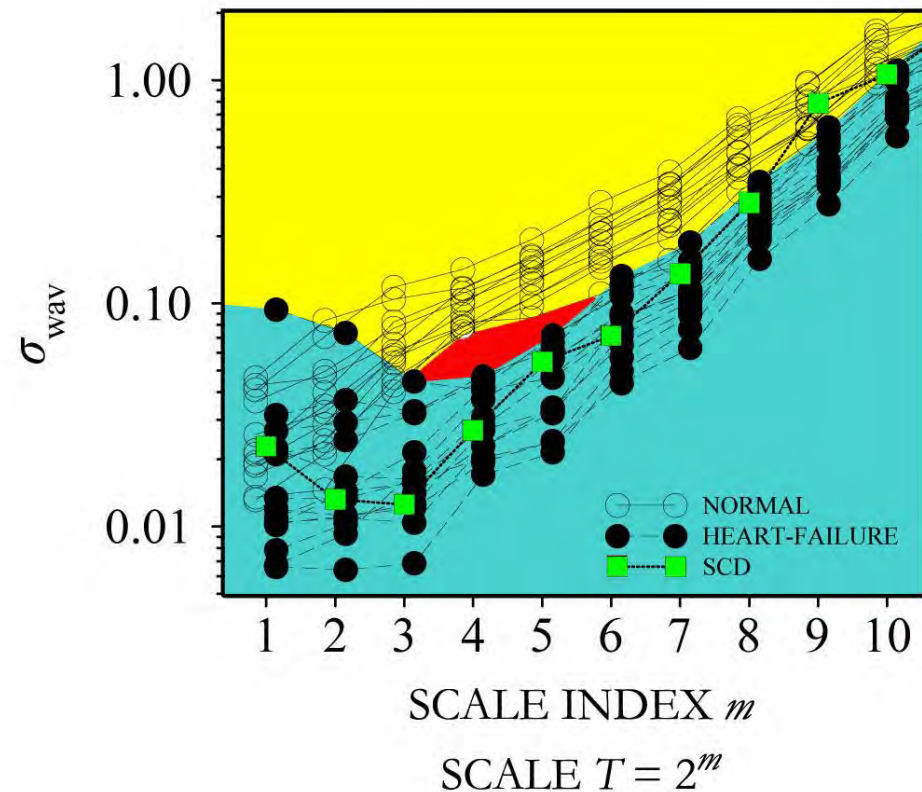


Daubechies

Haar wavelet

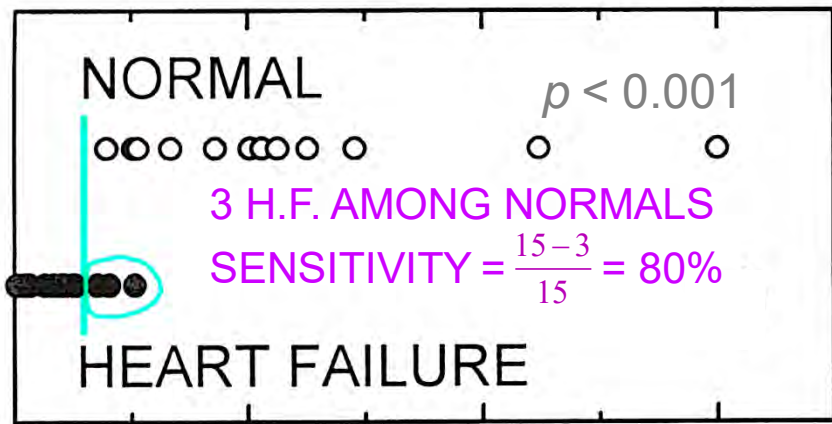


Daubechies 10-tap wavelet



S. Thurner, M. C. Feurstein, and M. C. Teich, "Multiresolution Wavelet Analysis of Heartbeat Intervals Discriminates Healthy Patients from Those with Cardiac Pathology," *Phys. Rev. Lett.* **80**, 1544-1547 (1998).

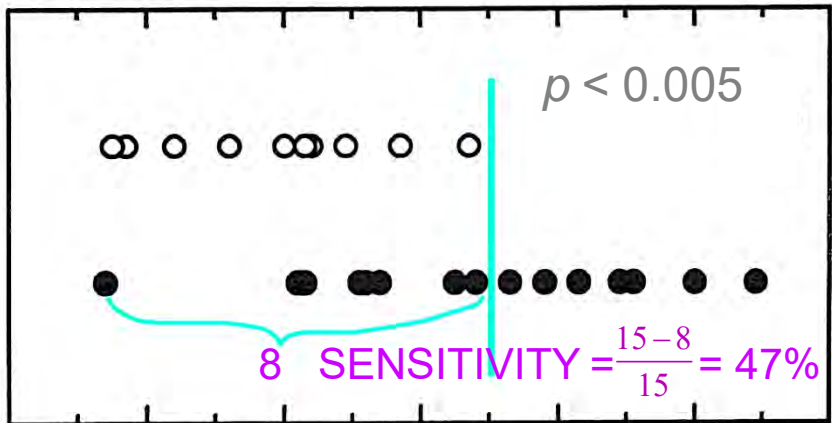
IDENTIFYING PATIENTS WITH CARDIAC DYSFUNCTION



0.00 0.02 0.04 0.06

Var(τ) (sec²)

SCALE-DEPENDENT



0.8 1.0 1.2 1.4 1.6 1.8 2.0

EXPONENT α_{St}

SCALE-INDEPENDENT

MEASURES OF STATISTICAL SIGNIFICANCE

- p VALUE, d' , AND VARIANTS (rely on Gaussian assumption)

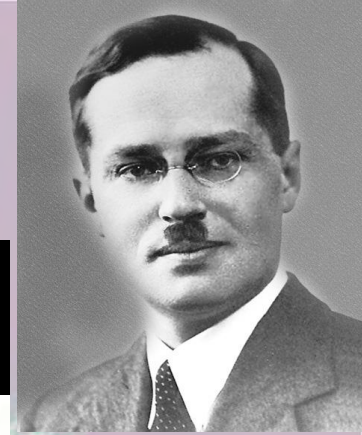
- SENSITIVITY/SPECIFICITY MEASURES OF CLINICAL SIGNIFICANCE (distribution free)

SENSITIVITY \equiv proportion of heart-failure patients that are properly identified

e.g., Hypothesis that all normal patients are so identified \equiv 100% SPECIFICITY

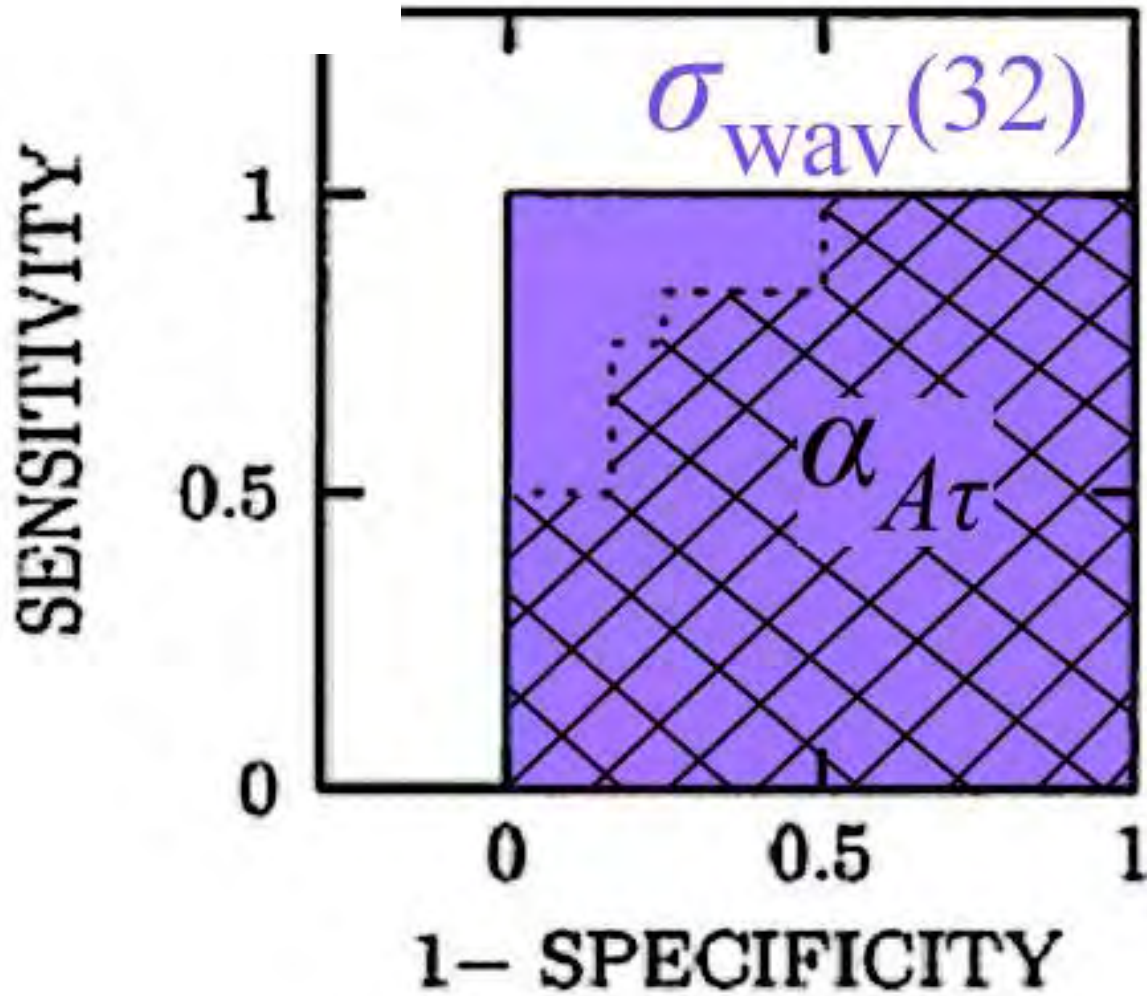
- ROC CURVES & AREA UNDER ROC

ROC CURVES & AREA UNDER ROC

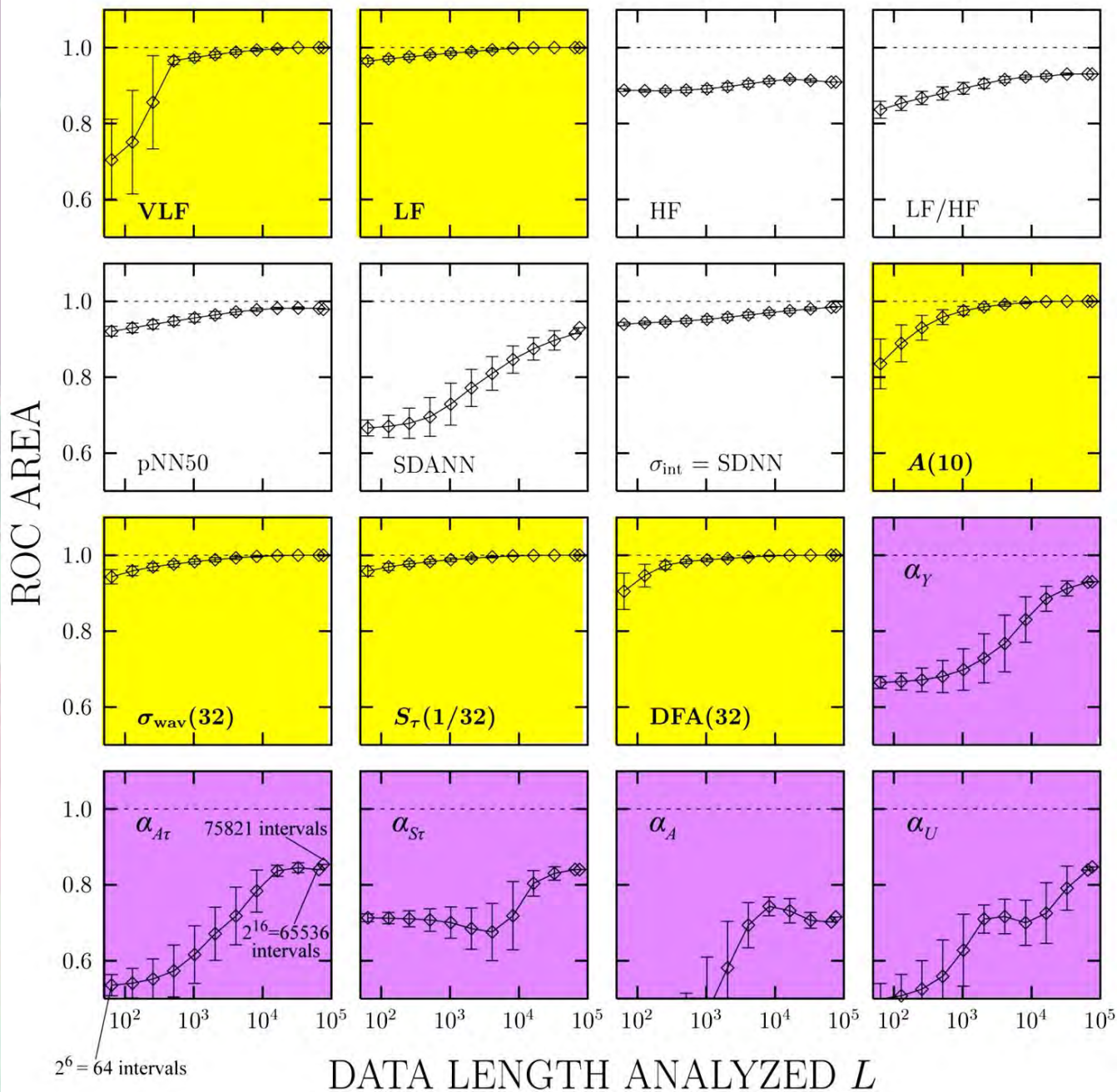


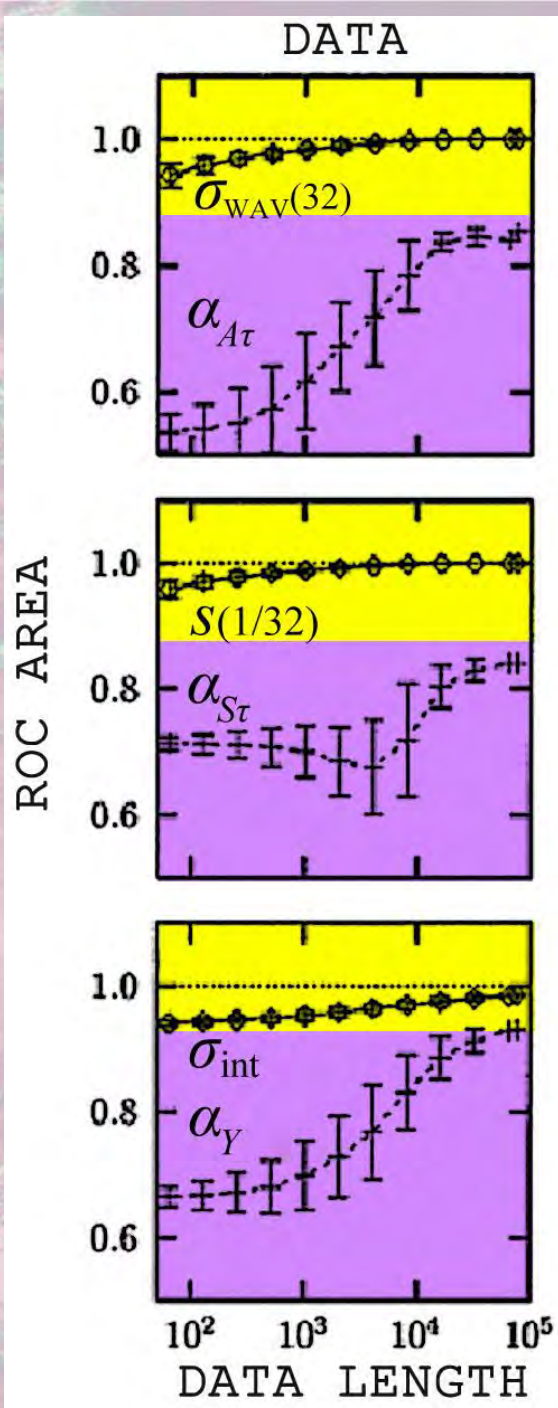
SCALE-DEPENDENT $\sigma_{\text{wav}}(32)$

SCALE-INDEPENDENT $\alpha_{A\tau}$

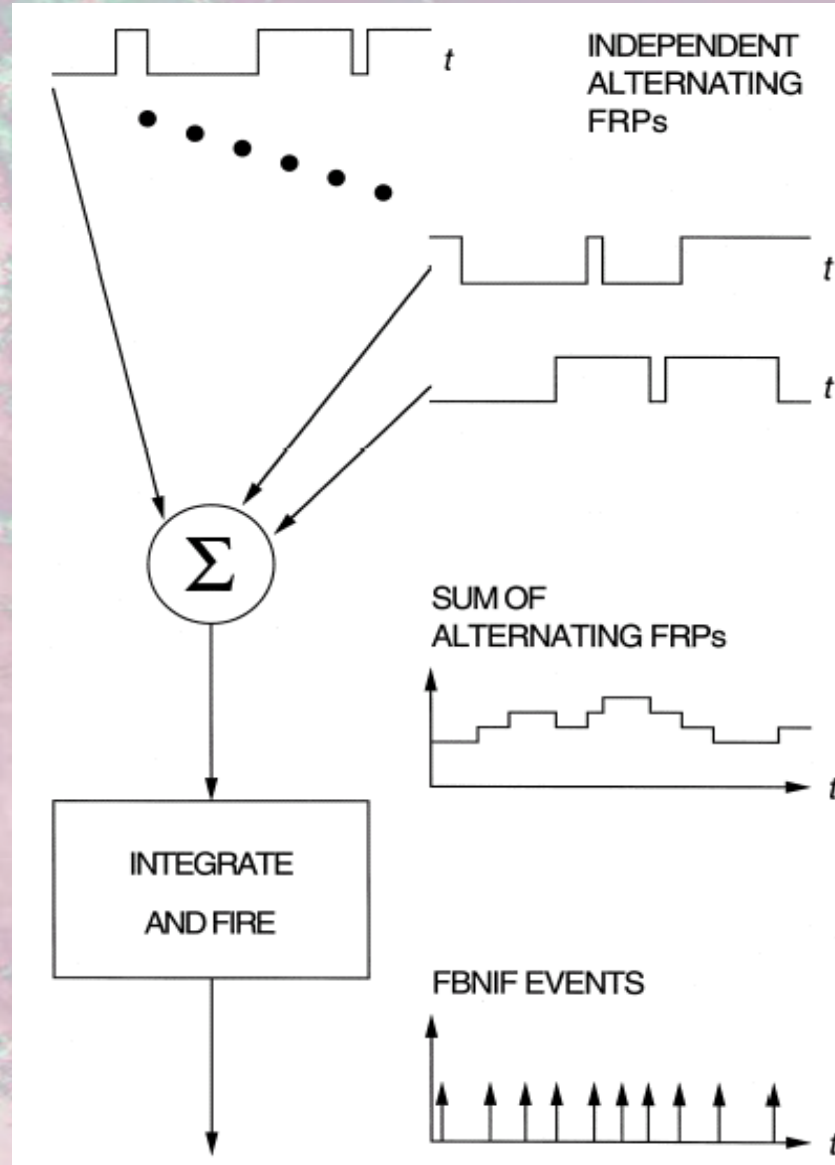
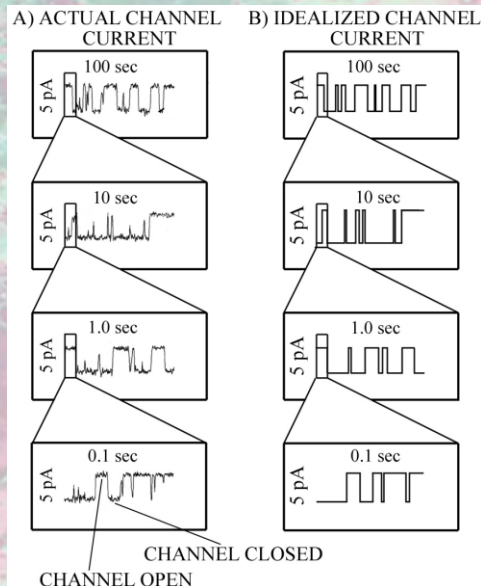
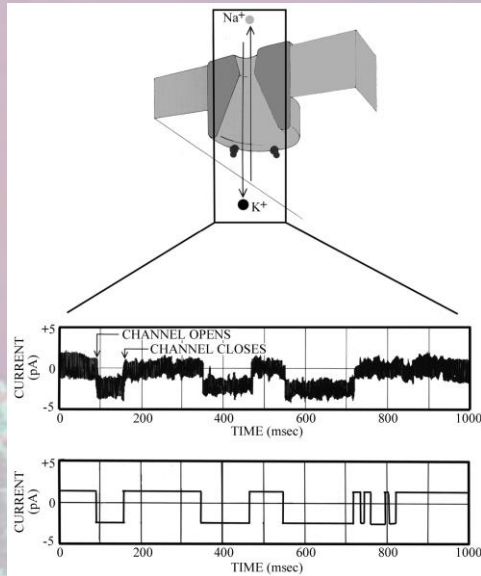


ROC-AREA CURVES: NORMAL & CHF DATA





PHYSIOLOGICAL ORIGIN OF FRACTAL BEHAVIOR



Bernoulli



Gauss



Kolmogorov

Lapicque



Adapted from S. Thurner, S. B. Lowen, M. Feurstein, C. Heneghan, H. G. Feichtinger, and M. C. Teich, "Analysis, Synthesis, and Estimation of Fractal-Rate Stochastic Point Processes," *Fractals* 5, 565-595 (1997).

6. NETWORKS

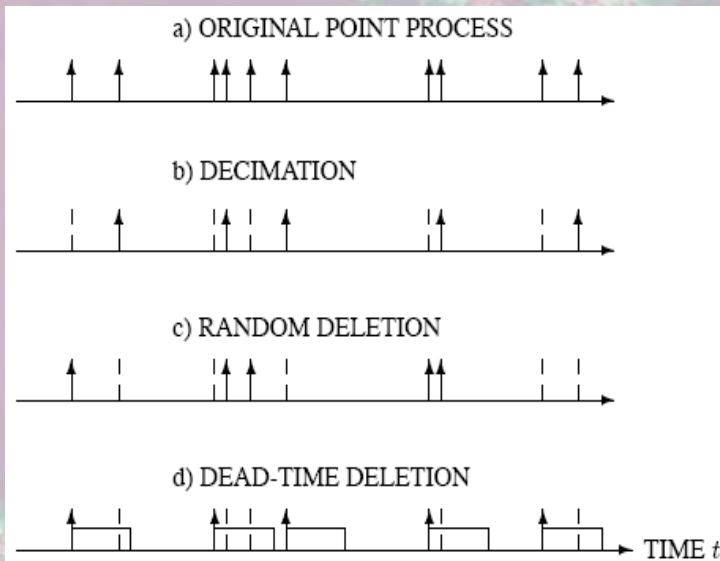
EXAMPLES OF SCALE-FREE NETWORKS

- Cellular metabolic networks
- Air transportation
- Internet
(as of 2005, >100,000 separate networks, >100 million hosts, millions of routers, billions of web locations, tens of billions of catalogued documents)
- Web
- Scientific collaborations (linked by joint publications)
- Scientific papers (linked by citations)
- People (connected by professional associations or friendships)
- Businesses (linked by joint ventures)

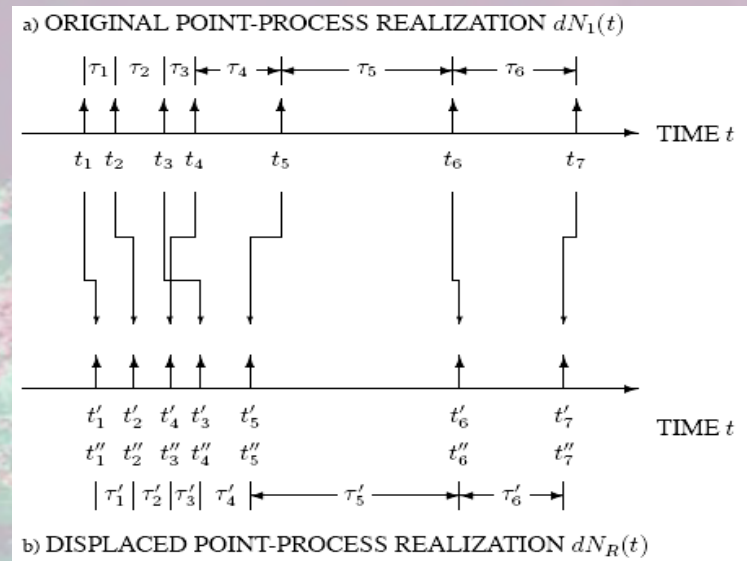
SUCH NETWORKS ARE ROBUST ABAINST ACCIDENTAL FAILURES
BECAUSE RANDOM BREAKDOWNS SELECTIVELY AFFECT THE MOST
PLENTIFUL NODES, WHICH ARE THE LEAST CONNECTED

SURROGATE DATA ANALYSIS

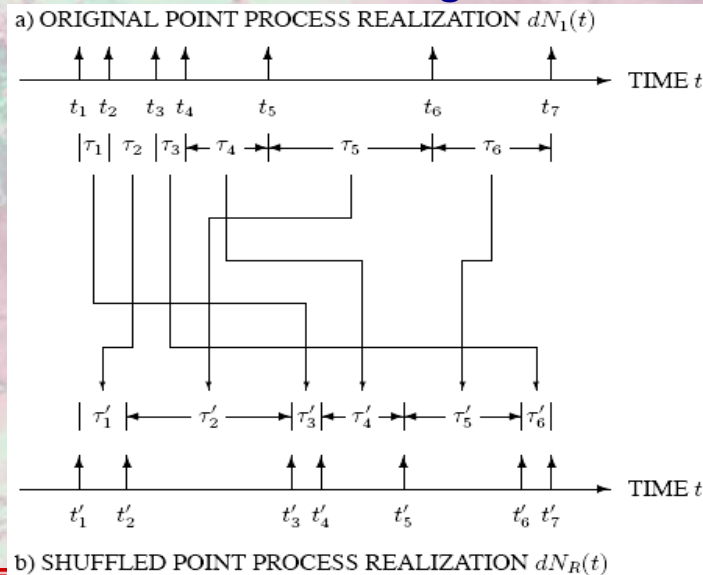
Deletion



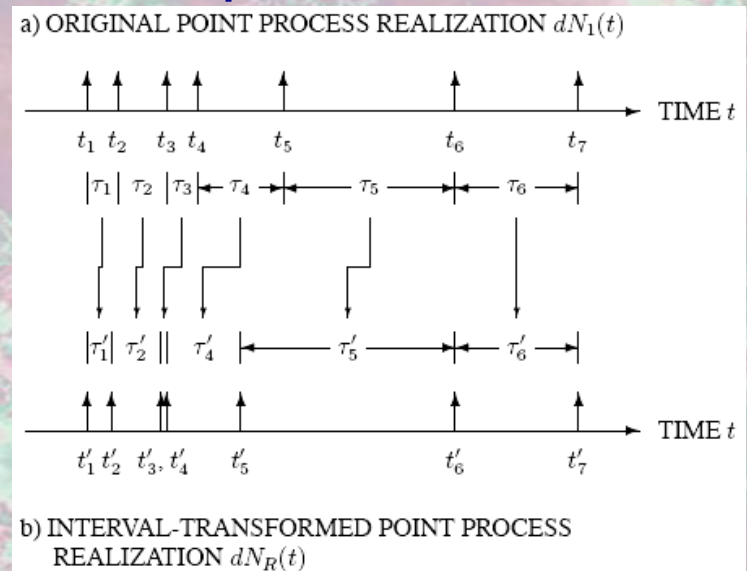
Displacement



Shuffling

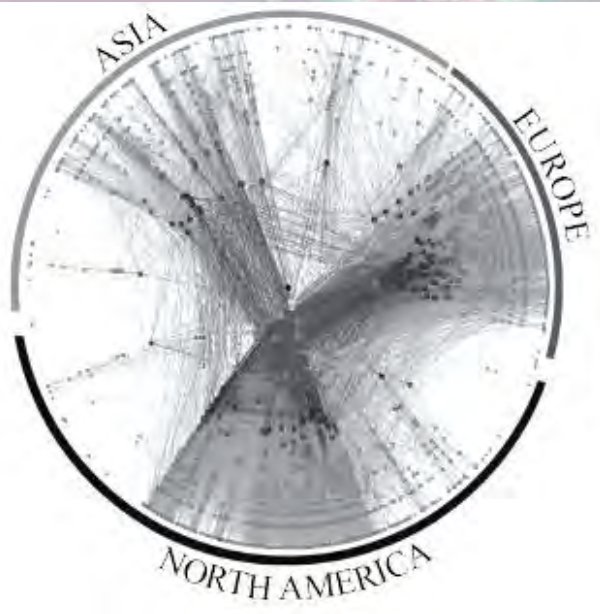


Exponentialization

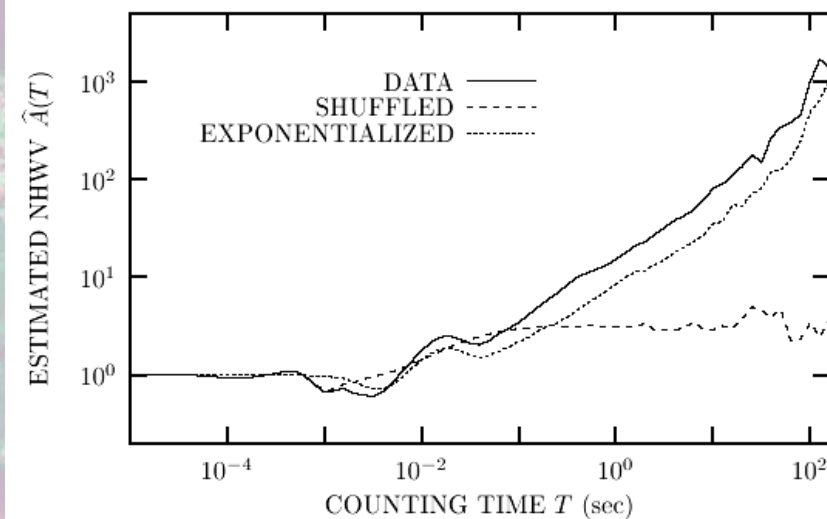


APPLICATIONS: COMPUTER NETWORK TRAFFIC

Snapshot of 11,000 ISPs from CAIDA (April/May 2003)



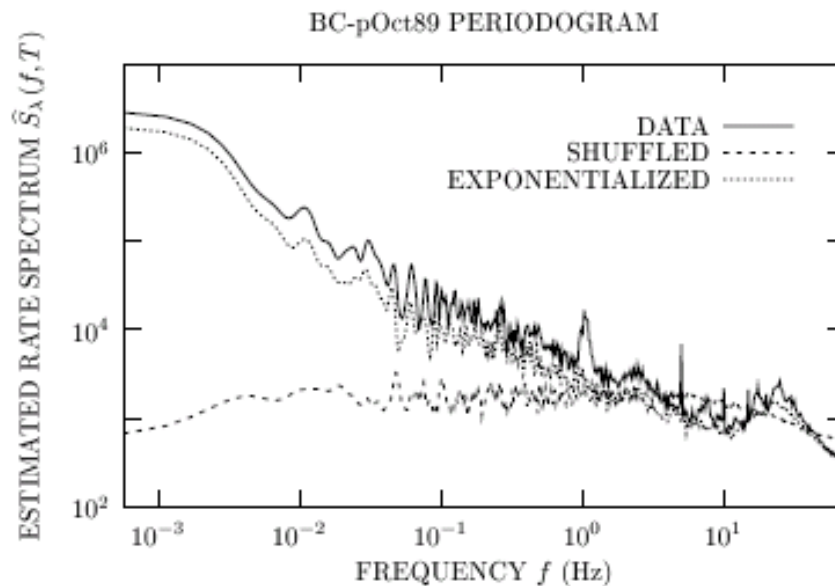
1 million consecutive Ethernet packet arrivals over 29 min (data set BC-pOct89)



Erlang



Palm



IDENTIFYING THE NETWORK-TRAFFIC POINT PROCESS

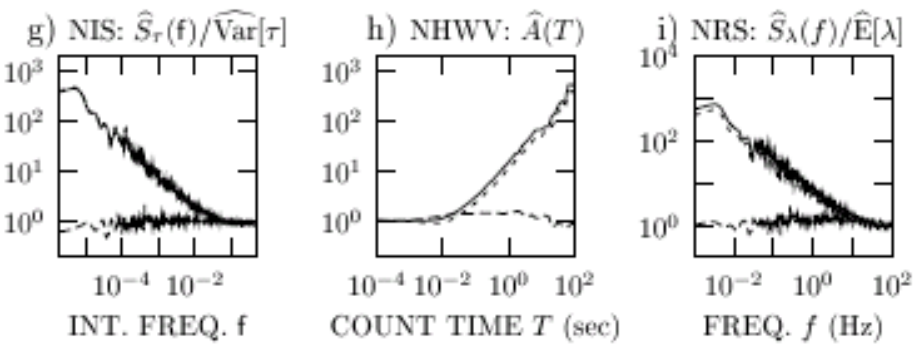
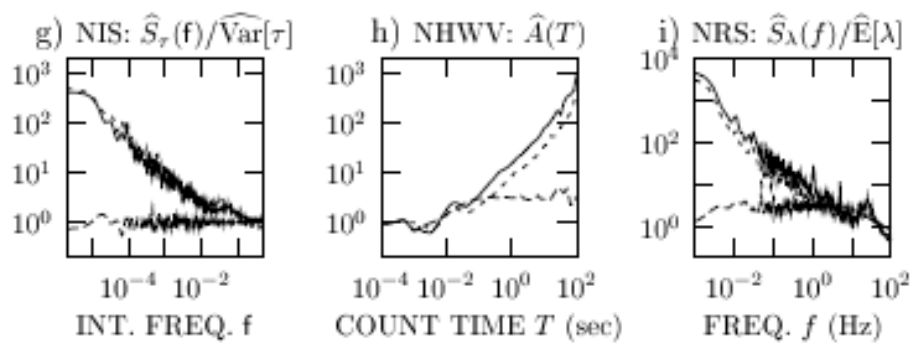
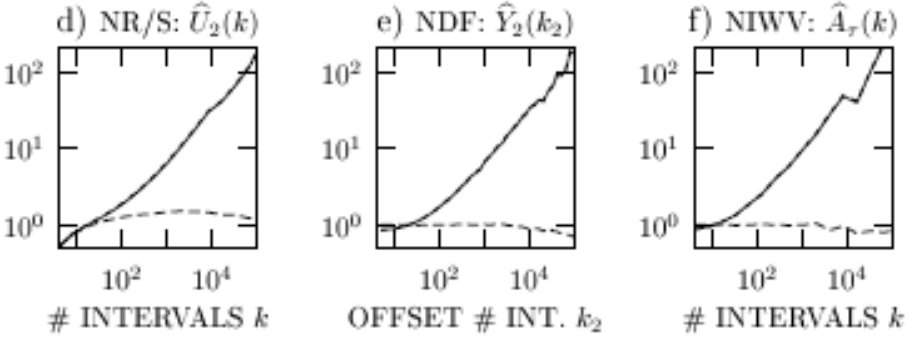
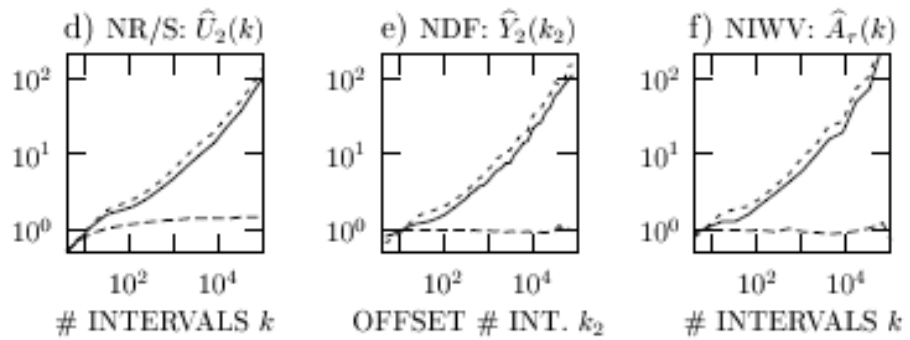
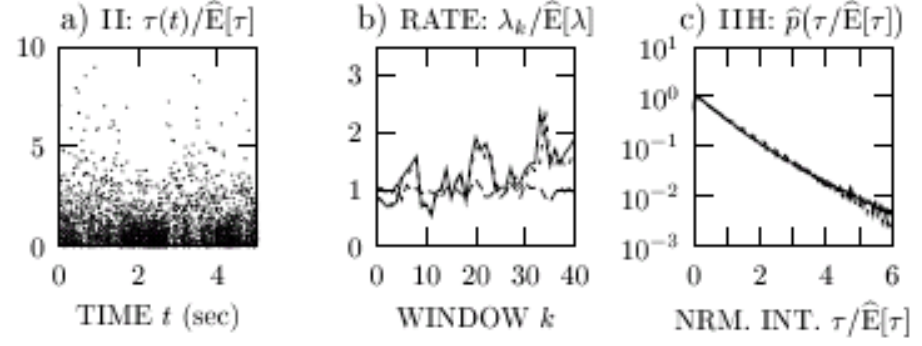
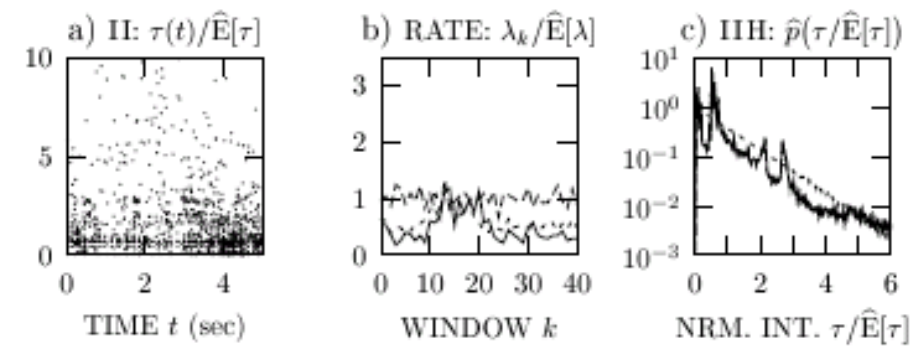
TABLEAU OF NINE STATISTICAL MEASURES

CLASSIC BC-pOct89 DATA SET

SIMULATED FRACTAL NEYMAN-SCOTT POINT PROCESS

1-million Consecutive Ethernet Packet Arrivals at Main Ethernet Cable

(Rectangular Fractal-Shot-Noise-Driven Point Process: RFSNDP)



— BC-pOct89
 --- SHUFFLED
 ---- EXPONENTIALIZED

— RFSNDP
 --- SHUFFLED
 ---- EXPONENTIALIZED

Table of Contents:

Preface.

List of Figures.

List of Tables.

Authors.

1. Introduction.

2. Scaling, Fractals, and Chaos.

3. Point Processes: Definition and Measures.

4. Point Processes: Examples.

5. Fractal and Fractal-Rate Point Processes.

6. Processes Based on Fractional Brownian Motion.

7. Fractal Renewal Processes.

8. Processes Based on the Alternating Fractal Renewal Process.

9. Fractal Shot Noise.

10. Fractal-Shot-Noise-Driven Point Processes.

11. Operations.

12. Analysis and Estimation.

13. Computer Network Traffic.

Appendix A: Derivations.

Appendix B: Problem Solutions.

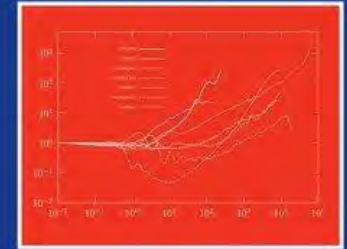
Appendix C: List of Symbols.

Bibliography.

Author Index.

Subject Index.

Fractal-Based Point Processes



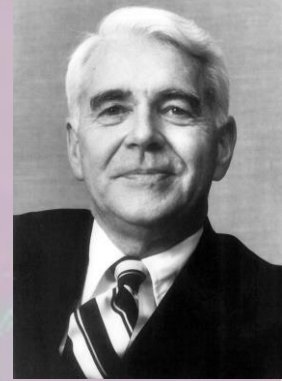
Steven Bradley Lowen
Malvin Carl Teich

www.
wiley.com

WILEY SERIES IN PROBABILITY AND STATISTICS



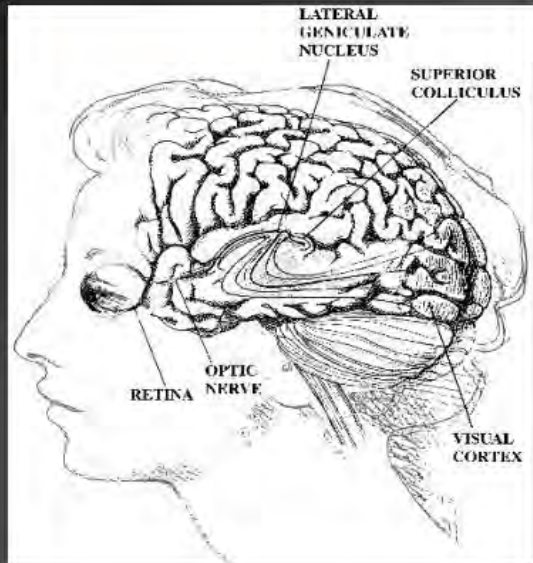
7. SENSORY DETECTION



McGill

SENSORY TRANSMISSION AND DETECTION

M. C. Teich & W. J. McGill

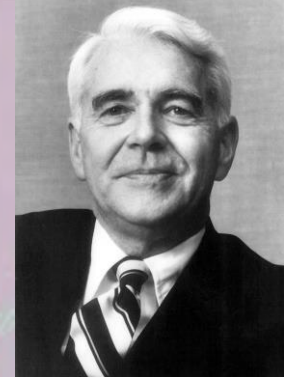


<http://people.bu.edu/teich>

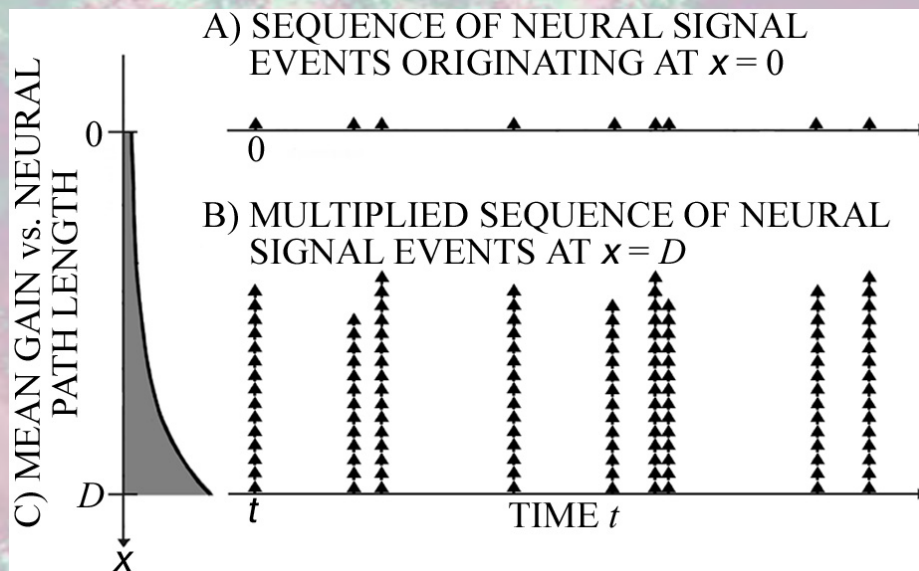
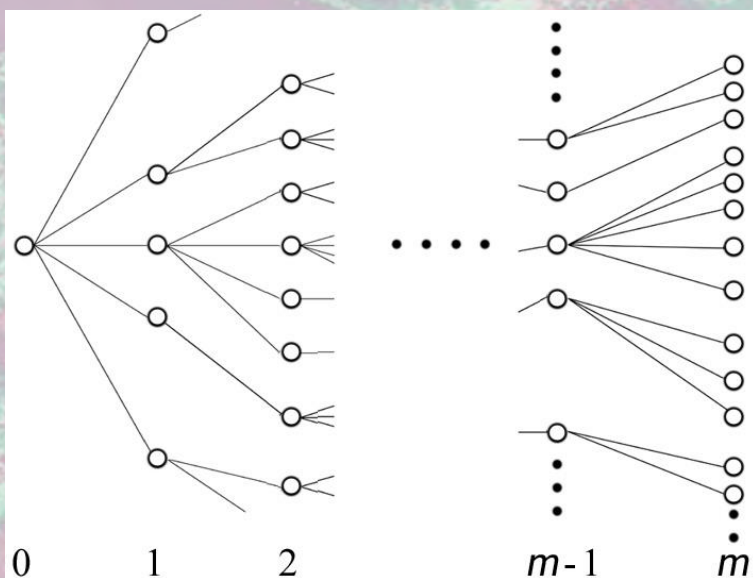
Alerting Signals and Detection in a Sensory Network

WILLIAM J. MCGILL[†] AND MALVIN C. TEICH[‡]

Columbia University



McGill



CORTICAL-ACTIVATION EXTENT VS. STIMULUS INTENSITY

VISUAL-CORTEX ACTIVATION EXTENT (UNIFORM FIELD)

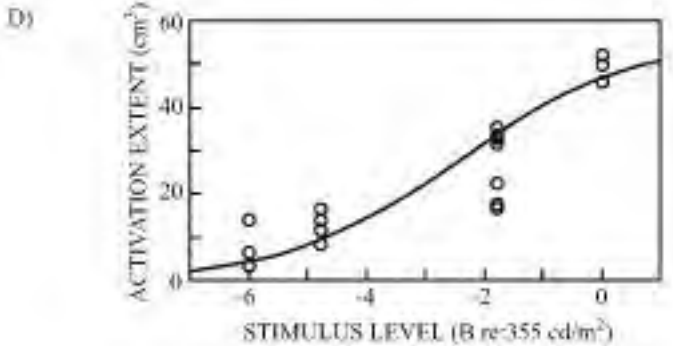
A) LOW INTENSITY (5.62 cd/m²)



B) HIGH INTENSITY (355 cd/m²)

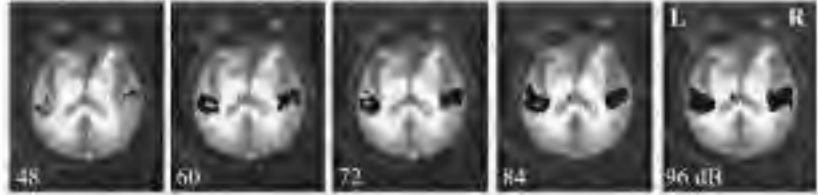


C) VISUAL AREAS

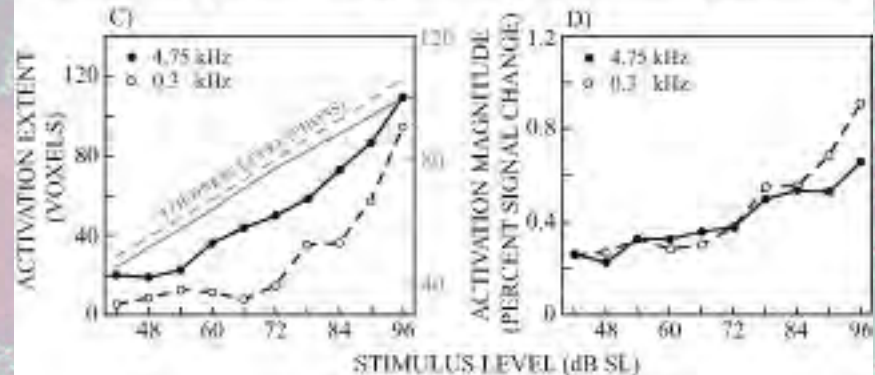
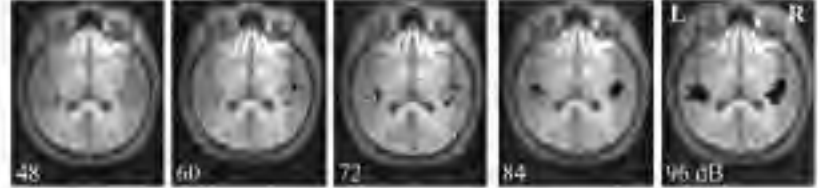


AUDITORY-CORTEX ACTIVATION EXTENT (TONE)

A) HIGH FREQUENCY (4.75-kHz TONE)



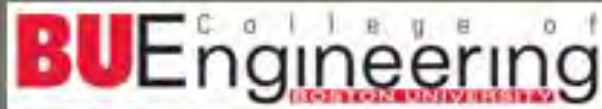
B) LOW FREQUENCY (0.3-kHz TONE)



Hart, Hall, and Palmer, "The Sound-Level-Dependent Growth in the Extent of fMRI Activation in Heschl's Gyrus is Different for Low- and High-Frequency Tones," *Hearing Res.* **179**, 104-112 (2003).

Aguirre, Komáromy, Cideciyan, Brainard, Aleman, Roman, Avants, Gee, Korczykowski, Hauswirth, Acland, Aguirre, and Jacobson, "Canine and Human Visual Cortex Intact and Responsive Despite Early Retinal Blindness from RPE65 Mutation," *PLoS Med.* **4**, 1117-1128 (2007).

SUPPORT GRATEFULLY ACKNOWLEDGED



The David and Lucile Packard Foundation

